

Mass Spectrometry of Nonmolecular Materials: ^{252}Cf -Plasma Desorption and Gas-Phase Clustering of Cadmium Thiolate Compounds

A. Grey Craig,^{*1} Keith J. Fisher,² Robert Garbutt,² Ian G. Dance,² and Peter J. Derrick³

The Clayton Foundation Laboratories for Peptide Biology, The Salk Institute, P.O. Box 85800, San Diego, California 92186-5800

Received February 15, 1994⁶

We report that eight cadmium arenethiolate compounds with general formula $^n[\text{Cd}(\text{SAr})_2]$ and cadmium phenylmethanethiolate $^n[\text{Cd}(\text{SBz})_2]$ (Bz = $\text{CH}_2\text{C}_6\text{H}_5$), when subjected to plasma desorption time-of-flight mass spectrometry, yield positive and negative ions up to 3.7 kDa. The spectra reveal extended series of ions containing both RS⁻ and S²⁻. For the Cd(SAr)₂ compounds (Ar = C₆H₅, C₆H₄-4-F, C₆H₄-4-Cl, C₆H₄-4-CH₃, C₆H₄-4-OCH₃, C₆H₄-4-C₄H₉, C₆H₄-2-CH₃) there occur sequences of positive ions $[\text{Cd}_x(\text{SAr})_{2x-1}]^+$ ($x = 1 - 8$), $[\text{Cd}_x\text{S}(\text{SAr})_{2x-3}]^+$ ($x = 2 - 6$), $[\text{Cd}_x\text{S}_2(\text{SAr})_{2x-5}]^+$ ($x = 3 - 7$), and $[\text{Cd}_x\text{S}_3(\text{SAr})_{2x-7}]^+$ ($x = 4, 5, 7$) and negative ions $[\text{Cd}_x\text{S}(\text{SAr})_{2x-1}]^-$ ($x = 1 - 3$), $[\text{Cd}_x\text{S}_2(\text{SAr})_{2x-3}]^-$ ($x = 2 - 4$), and $[\text{Cd}_x\text{S}_3(\text{SAr})_{2x-5}]^-$ ($x = 3, 4$): not all ions are observed for all compounds, and other ions involving fragmentation of SAr are also present. A quite different array of ions occurs for Cd(SBz)₂. In the positive ion spectrum, 21 of the 24 ions fall into three series: $[\text{Cd}_x\text{S}_{x-1}(\text{SBz})]^+$ ($x = 2, 3$); $[\text{Cd}_x\text{S}_{x-2}(\text{SBz})_3]^+$ ($x = 2 - 8, 10 - 12$); $[\text{Cd}_x\text{S}_{x-3}(\text{SBz})_5]^+$ ($x = 3 - 11$). The negative ions for Cd(SBz)₂ also fit three series: $[\text{Cd}_x\text{S}_x(\text{SBz})]^-$ ($x = 1 - 13$); $[\text{Cd}_x\text{S}_{x-1}(\text{SBz})_3]^-$ ($x = 1, 2, 3$); $[\text{Cd}_x\text{S}_{x-3}(\text{SBz})_6]^-$ ($x = 3 - 5, 7 - 9$). The occurrence of these series, the absence of preferred numbers of Cd atoms, and an absent preference for $x = 4$ ions from the solids known to contain linked Cd₄ (adamantanoid) cages all indicate that the ions are formed not simply by excision from the solids. The ion distributions are interpreted in terms of processes which are probably associative during the initial formation of an energetic ion aggregate but are evidently dissociative from this intermediate. A staircase structural motif involving Cd₂{SR₂}₂ rhombuses sharing *trans* edges is proposed to account for the compositions and transformations of the series of ions.

Introduction

The advances made in the development of ionization techniques allow for mass spectrometric analysis of a wide range of biological samples.⁴ Such thermally labile compounds were once thought of as mass-spectrometrically intractable substances because of the difficulty of appropriately transferring energy to relatively large molecules to facilitate desorption/ionization. Plasma desorption (PD) time-of-flight mass spectrometry addresses this problem by bombarding the sample with high energy particles, typically fission fragments from the ^{252}Cf nuclide.⁵

The successful analysis of a variety of proteins above 20 kDa is evidence of the ability of PD to transfer energy to a molecule to overcome barriers to desorption without exceeding the internal bond dissociation energies of the molecules. The mass spectrometric investigation of a nonmolecular solid, however, is quite a different experiment, since by definition bonds must be broken in order to release parts of the structure into the gas phase. This could happen in many ways, and the resulting fragments would presumably have dangling peripheral bonds unless modified by structural rearrangement. Depending on the amount of rearrangement, the desorbed fragments might or might not reflect the structure of the solid state.

To date, the only nonmolecular compounds studied extensively by mass spectrometry are the elements themselves and binary compounds such as alloys, metal halides, oxides, and sulfides.⁶⁻¹²

In general, well developed series of ions appear, and at least in the case of binary halides the compositions of the prominent ion series can be rationalized in terms of symmetrical fragments of the solid-state structure. In all of these systems the density of bonds of the structures in the solid state is high. The application of PD to these materials is limited to studies of single metal¹³⁻¹⁵ or polymetal¹⁶⁻¹⁹ complexes. In contrast to the large (CsI)_nCs⁺ clusters containing hundreds of atoms produced when CsI is bombarded with relatively low energy (5 keV) xenon ions,²⁰ PD typically produces only small clusters of up to 10 atoms.²¹

In this paper, we report the PD mass spectra of a new and different class of compound, in which the crystal phase is structurally nonmolecular but is composed of large quasi-molecular units connected by a relatively small proportion of bonds. Consequently, the density of bonds to be disrupted for the

* Author to whom correspondence should be addressed.

⁶ Abstract published in *Advance ACS Abstracts*, May 1, 1994.

(1) The Salk Institute.

(2) Present address: School of Chemistry, University of New South Wales, P.O. Box 1, Kensington, 2033 NSW, Australia.

(3) Present address: Warwick Institute of Mass Spectrometry and Department of Chemistry, University of Warwick, Coventry CV4 7AL, U.K.

(4) Delgass, W. N.; Cooks, R. G. *Science* **1987**, *23*, 545–552.

(5) Sundqvist, B.; Macfarlane, R. D. *Mass Spectrom. Rev.* **1985**, *4*, 421–460.

(6) Martin, T. P. *Angew. Chem.* **1986**, *25*, 197–296.

(7) Gord, J. R.; Bemish, R. J.; Freiser, B. S. *Int. J. Mass Spectrom. Ion Processes* **1990**, *102*, 115–132.

(8) Parent, D. C. *Chem. Phys. Lett.* **1991**, *183*, 51–54.

(9) El Nakat, J. H.; Dance, I. G.; Fisher, K. J.; Rice, D.; Willett, G. D. *J. Am. Chem. Soc.* **1991**, *113*, 5141–5148.

(10) El Nakat, J. H.; Dance, I. G.; Fisher, K. J.; Willett, G. D. *Inorg. Chem.* **1991**, *30*, 2957–2958.

(11) El Nakat, J. H.; Dance, I. G.; Fisher, K. J.; Willett, G. D. *J. Chem. Soc., Chem. Commun.* **1991**, 746–748.

(12) El Nakat, J. H.; Fisher, K. J.; Dance, I. G.; Willett, G. D. *Inorg. Chem.* **1993**, *32*, 1931–1940.

(13) Pannell, L. K.; Fales, H. M.; Scovill, J. P.; Klayman, D. L.; West, D. X.; Tate, R. L. *Transition Met. Chem. (Weinheim, Ger.)* **1985**, *10*, 141–147.

(14) van Veelen, P. A. *Org. Mass Spectrom.* **1991**, *26*, 74.

(15) Allmaier, G.; Roepstorff, P.; Schwarzhans, K. E.; Utri, G. *Rapid Commun. Mass Spectrom.* **1992**, *6*, 58–61.

(16) Fackler, J. P. J.; McNeal, C. J.; Winpenny, R. E. P.; Pignolet, L. H. *J. Am. Chem. Soc.* **1989**, *111*, 6434–6435.

(17) Da Silveira, E. F.; Mcafee, C. D.; Cocke, D. L.; Naugle, D. G.; Sun, D.; Schweikert, E. A. *Int. J. Mass Spectrom. Ion Processes* **1989**, *91*, R5–R11.

(18) Utri, G.; Schwarzhans, K.-E.; Allmaier, G. M. *Z. Naturforsch.* **1990**, *45B*, 755–762.

(19) McNeal, C. J.; Hughes, J. M.; Lewis, G. J.; Dahl, L. F. *J. Am. Chem. Soc.* **1991**, *113*, 372–373.

(20) Barlak, T. M.; Wyatt, J. R.; Colton, R. J.; DeCorpo, J. J.; Campana, J. E. *J. Am. Chem. Soc.* **1982**, *104*, 1212–1215.

(21) Kamensky, I.; Håkansson, P.; Sundqvist, B.; McNeal, C. J.; Macfarlane, R. *Nucl. Instrum. Methods* **1982**, *198*, 65–68.

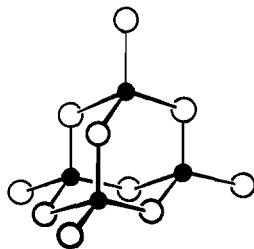


Figure 1. Adamantoid cage. This is the repeating structural unit in $\text{Cd}(\text{SPh-4-Me})_2$ where Cd atoms are represented with closed circles and SPh-4-Me with open circles.

release of molecular fragments is low. These crystal structures are found in the cadmium arenethiolates, ${}^n[\text{Cd}(\text{SAR})_2]$ (the notation n describes infinite connectivity in n dimensions), whose simple general formula belies their complex and filigreed structures. The specific cadmium arenethiolate compounds studied are as follows: 1, Ar = C_6H_5 ; 2, Ar = $\text{C}_6\text{H}_4\text{-4-F}$; 3, Ar = $\text{C}_6\text{H}_4\text{-4-Cl}$; 4, Ar = $\text{C}_6\text{H}_4\text{-4-CH}_3$; 5, Ar = $\text{C}_6\text{H}_4\text{-4-OCH}_3$; 6, Ar = $\text{C}_6\text{H}_4\text{-4-C}_6\text{H}_5$; 7, Ar = $\text{C}_6\text{H}_4\text{-2-CH}_3$; and 8, Ar = C_6F_5 . We have also investigated bis(phenylmethanethiolato)cadmium, 9, $\text{Cd}(\text{SBz})_2$ (Bz = $\text{CH}_2\text{C}_6\text{H}_5$), which is chemically different and for which the crystal structure is unknown although almost certainly nonmolecular.

Samples 1, 2, 4, and 7 have been crystallized and shown using X-ray structure determination to be nonmolecular in three dimensions.^{22–25} The crystal structures of 1, 2, and 4 contain the adamantoid cage (see Figure 1) as the repeating structural unit. The core of this cage contains four cadmium atoms arrayed as a tetrahedron and linked by six doubly-bridging arenethiolate ligands arrayed as an octahedron. Four more peripheral arenethiolate ligands complete the tetrahedral coordination at the cadmium atoms. The adamantoid cage is a paradigmatic structural unit in many crystalline molecular and nonmolecular metal thiolates and sulfides^{26–31} and is well established as a molecular species in $[\text{Cd}_4(\text{SPh})_{10}]^{2-}$ (Ph = C_6H_5) and many derivatives.^{27,32,33} In crystalline 1, 2, and 4 each adamantoid cage shares its terminal thiolate ligands with neighboring adamantoid cages, and therefore the structural formula of these three compounds is ${}^n\{(\mu\text{-SAR})_6\text{Cd}_4(\mu\text{-SAR})_{4/2}\}$. The crystal structures thus contain intracage Cd–S bonds and intercage Cd–S bonds in a 12:4 ratio. The arrangement of the tetrahedral adamantoid cages in 1 and 2 is the same as that of the SiO_4 tetrahedra in the α -cristobalite lattice of SiO_2 .^{22,23} However, in 4 the adamantoid cages are connected to enclose large cavities (see Figure 1) and channels and resemble enlarged zeolite lattices. The crystal structure of 7 is composed of spiro-linked $\{\text{Cd}_2(\mu\text{-SAR})_2\}$ and $\{\text{Cd}_3(\mu\text{-SAR})_3\}$ cycles and contains solvent DMF (*N,N*-dimethylformamide) weakly coordinated to three Cd atoms of

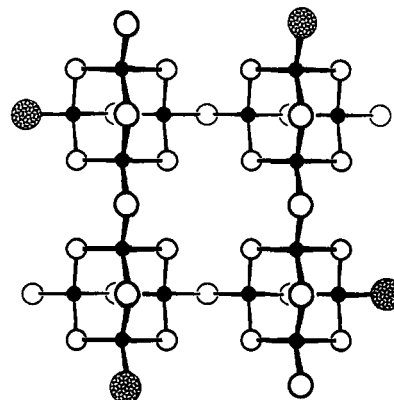


Figure 2. $\{\text{Cd}_{16}(\text{SAR})_{32}\text{L}_4\}$ structure with four linked adamantoid cages. Closed circles are Cd; open circles are SAR; the large shaded circles are the four peripheral heteroligands.

the latter cycle.²⁵ DMF coordination occurs also in $\text{Cd}_8(\text{SC}_6\text{H}_4\text{-Br-4})_{16}(\text{DMF})_3$, which has adamantoid cages linked in a two dimensional network.²⁴ The crystal structures of 3, 5, 6, and 8 are not yet known.

This picture of the Cd–S framework, in which one-third of the Cd–S bonds are responsible for the nonmolecularity, is misleading, because the Ar substituents connected to the S atoms occupy most of the volume of the crystals. Thus in 1 the crystal volume is composed of approximately 12% CdS framework, 80% C_6H_5 substituents, and 8% void. In 4 the S···S diagonals of the cavity shown in Figure 1 are 16–19 Å in length. The number density of the Cd–S bonds that link the adamantoid cages in 1 is only 12 per 5000 Å³. In the solid state these compounds are very different from the binary inorganic compounds that have dominated most mass spectrometric investigations of nonmolecular solids to date.

The arenethiolates compounds 1–7 and the phenylmethanethiolate 9 dissolve in weakly donor solvents such as DMF or dimethyl sulfoxide (but not in other solvents), from which it is inferred that on dissolution the nonmolecular crystal structure is disrupted by partial coordination of the solvent. We have used ¹¹³Cd and ¹³C nuclear magnetic resonance to probe the nature of the species in DMF solutions of 1, 2 and 4, with the conclusion that there exist series of macromolecules composed of vertex-linked adamantoid tetrahedra, such as that shown in Figure 2, with some DMF coordination at peripheral positions.³⁴ In summary, the crystal structures of these compounds, their ease of dissolution, and the probable molecular structures in solution combine to suggest facile desorption of molecular ions with adamantoid or related structures from the solids. In preliminary investigations of compound 4 using PD, we observed a number of series of fragment ions which we tentatively assigned.³⁵ Recently, we have further clarified the composition of several of the fragment clusters formed for compound 2.³⁶ On the basis of the spectra of compounds 1–9, we sought to verify the identity of the fragment ion series previously identified and thereby investigate the gas phase ions formed by PD. The only other mass spectra reported for compounds of this type are by neutral LSIMS on $\text{Cd}_2(\text{SPh})_4(\text{PPh}_3)$,³⁷ SIMS and PDMS on four nickel alkanethiolates with cyclic molecular structures $\text{Ni}_4(\text{SR})_8$, $\text{Ni}_6(\text{SR})_{12}$ and $\text{Ni}_8(\text{SR})_{16}$.³⁸ El Nakat et al. have measured laser desorption mass spectra of cadmium thiolates.³⁹

- (22) Dance, I. G.; Garbutt, R. G.; Craig, D. C.; Scudder, M. L. *Inorg. Chem.* **1987**, *26*, 4057–4064.
 (23) Craig, D. C.; Dance, I. G.; Garbutt, R. G. *Angew. Chem., Int. Ed. Engl.* **1986**, *25*, 165.
 (24) Dance, I. G.; Garbutt, R. G.; Craig, D. C.; Scudder, M. L.; Bailey, T. D. *J. Chem. Soc., Chem. Commun.* **1987**, 1164–1167.
 (25) Dance, I. G.; Garbutt, R. G.; Scudder, M. L. *Inorg. Chem.* **1990**, *29*, 1571–1575.
 (26) Krebs, B. *Angew. Chem. Int. Ed. Engl.* **1983**, *22*, 95–113.
 (27) Dance, I. G. *Polyhedron* **1986**, *5*, 1037–1104.
 (28) Blower, P. J.; Dilworth, J. R. *Coord. Chem. Rev.* **1987**, *76*, 121.
 (29) Krebs, B.; Henkel, G. In *Rings, Clusters and Polymers of Main Group and Transition Elements*; Roesky, H. W., Ed.; Elsevier: Amsterdam, 1989; pp 439–502.
 (30) Dance, I. G.; Fisher, K.; Lee, G. S. H. In *Metal Binding in Sulfur-Containing Proteins*; Stillman, M. J., Shaw, C. F., III, Suzuki, K. T., Eds.; VCH Publishers: New York, 1992; Vol. 22; pp 1794–1797.
 (31) Bedard, R. L.; Wilson, S. T.; Vail, L. D.; Bennett, J. M.; Flanigen, E. M. In *Zeolites: Facts, Figures, Future*; Jacobs, P. A., van Santen, R. A., Eds.; 1989; pp 375–387.
 (32) Hagen, K. S.; Holm, R. H. *Inorg. Chem.* **1983**, *22*, 3171–3174.
 (33) Hagen, K. S.; Stephan, D. W.; Holm, R. H. *Inorg. Chem.* **1982**, *21*, 3928–3936.

- (34) Dance, I. G.; Garbutt, R. G.; Bailey, T. D. *Inorg. Chem.* **1990**, *29*, 603–608.
 (35) Craig, A. G.; Kamensky, I.; Garbutt, R.; Dance, I. G.; Derrick, P. J. *Int. J. Mass Spectrom. Ion Processes* **1988**, *86*, 273–286.
 (36) Craig, A. G.; Kinny, D.; Garbutt, R.; Dance, I. G.; Derrick, P. J. *Org. Mass Spectrom.* **1992**, *27*, 1017–1029.
 (37) Black, S. J.; Einstein, F. W. B.; Hayes, P. C.; Kumar, R.; Tuck, D. G. *Inorg. Chem.* **1986**, *25*, 4181–4184.
 (38) Feld, H.; Leute, A.-L.; Rading, D.; Benninghoven, A.; Henkel, G.; Kruger, T.; Krebs, B. *Z. Naturforsch.* **1992**, *47B*, 929–936.

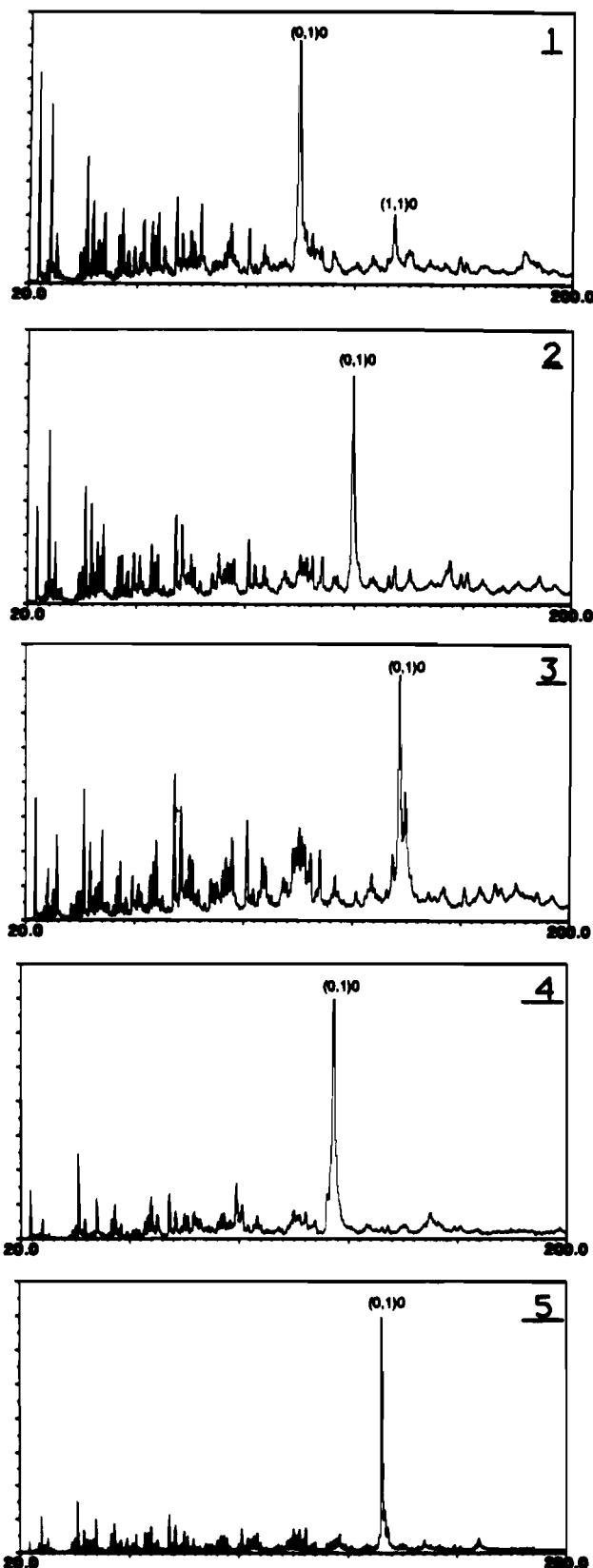


Figure 3. Low mass range of the positive PDMS spectra of compounds 1–5.

Experimental Section

The spectra shown in Figures 3–10 were measured using a BIOION 20 (Applied Biosystems AB Uppsala, Sweden), and a prototype extended flight path (EFP) PD time-of-flight mass spectrometer as described

(39) El Nakat, J. H.; Fisher, K. J.; Dance, I. G.; Willett, G. D. Unpublished results.

previously.⁴⁰ Accelerating voltages in the ranges +20 to +16 kV and –14 to –12 kV were used. Spectra were accumulated for periods of between 1 million primary ion events (8 min) and 100 million primary ion events (14 h). The BIOION 20 instrument had a 15-cm flight path, and the EFP instrument had a variable flight path that was set at either 31, 55, or 140 cm. To improve transmission in the EFP instrument, an electrostatic particle guide consisting of 10- μ m stainless steel wire held at ± 20 V potential and centered on the axis of the tube was used.^{40,41}

An aliquot (5 μ L) from a saturated solution of the compound in DMF or DMSO was electrosprayed (for between 3 and 5 min) onto thin mylar aluminized foils. An alternative sample preparation involved depositing an aliquot (5 μ L) of the above solution onto a nitrocellulose coated mylar foil. The solution was removed from the nitrocellulose surface immediately with a stream of nitrogen gas. The preparation of nitrocellulose foils has previously been detailed.⁴⁰

The spectra were calibrated using H^+/Na^+ in the positive mode and H^-/CN^- or H^-/HS_3^- in the negative mode. The masses of the observed fragments were defined as the middle of the fragment ion peak at approximately half-peak height. This procedure leads to an average mass, that should be compared to the chemical relative molecular mass of a proposed species. In those cases in which the isotopic cluster was resolved, the most intense fragment ion (indicated in the tables by an asterisk after the mass) was considered, and should be compared with the calculated mass of the most intense isotopomer. The mass accuracy of the PDMS technique is dependent on, among other factors, the contribution of metastable decomposition to the measured peak shape. The BIOION 20 instrument when used for the analysis of peptides and small proteins has a mass accuracy of $\pm 0.1\%$ for intact molecule ions⁴⁰ and $\pm 0.3\%$ for peptide fragment ions⁴² and resolution of ≈ 500 .⁴⁰ Using the EFP instrument, both the mass accuracy^{41,43} and the resolution^{36,40} improve considerably compared with the BIOION 20 instrument.

Results

Figures 3–10 show the PDMS spectra of compounds 1–9 over three linear mass ranges in (a) the positive and (b) the negative ionization mode. Tables 1–9 contain, for each compound, the observed masses and intensities for the positive and negative ions, together with calculated masses for the proposed assignments. Peaks in Figures 3–10 which have not been included in the tables are marked with an “x” above the peak, and are regarded as background peaks. The fragment intensities (s = strong, m = medium, and w = weak) indicate the intensity of each of the peaks relative to the surrounding peaks over the mass ranges displayed in Figures 3–10.

Many of the ions have the general formulation $[Cd_x S_m(SAr)_{2x+n}]$ (where the symbol Ar also includes the Bz substituent of 9) in which x is the number of cadmium atoms, m denotes the number of sulfide ions (S^{2-}), and n expresses the deviation of the SAR content from that in the precursor formula $Cd(SAr)_2$. In the figures, tables, and text discussion, the abbreviation $(m,n)_x$ is used for the composition $[Cd_x S_m(SAr)_{2x+n}]$.

Reproducibility of the Mass Spectra. All spectra presented in Figures 3–10 were measured with the electrospray sample preparation with the exception of the negative spectrum of compound 4 which was measured on nitrocellulose. The negative spectrum of compound 4, measured with the electrospray sample preparation, has previously been reported.³⁵ The relative intensities of the strong and medium intensity fragment ions observed in the spectra were found to be very reproducible for the same sample solution applied to several different targets. However, some small differences were observed in the intensities of weak fragment ions between successive targets analyzed at different times. These differences did not correlate with the duration of time the sample was exposed to the ^{252}Cf irradiation. Significant background peaks were observed when the mylar surface was not

(40) Kamensky, I.; Craig, A. G. *Anal. Instrum.* **1987**, *16*, 71–91.

(41) Craig, A. G.; Bennich, H.; Derrick, P. J. *Aust. J. Chem.* **1992**, *45*, 403–416.

(42) Craig, A. G. *Biol. Mass Spectrom.* **1991**, *20*, 195–202.

(43) Roepstorff, P.; Nielsen, P. F.; Kamensky, I.; Craig, A. G.; Self, R. *Biomed. Mass Spectrom.* **1988**, *15*, 305–310.

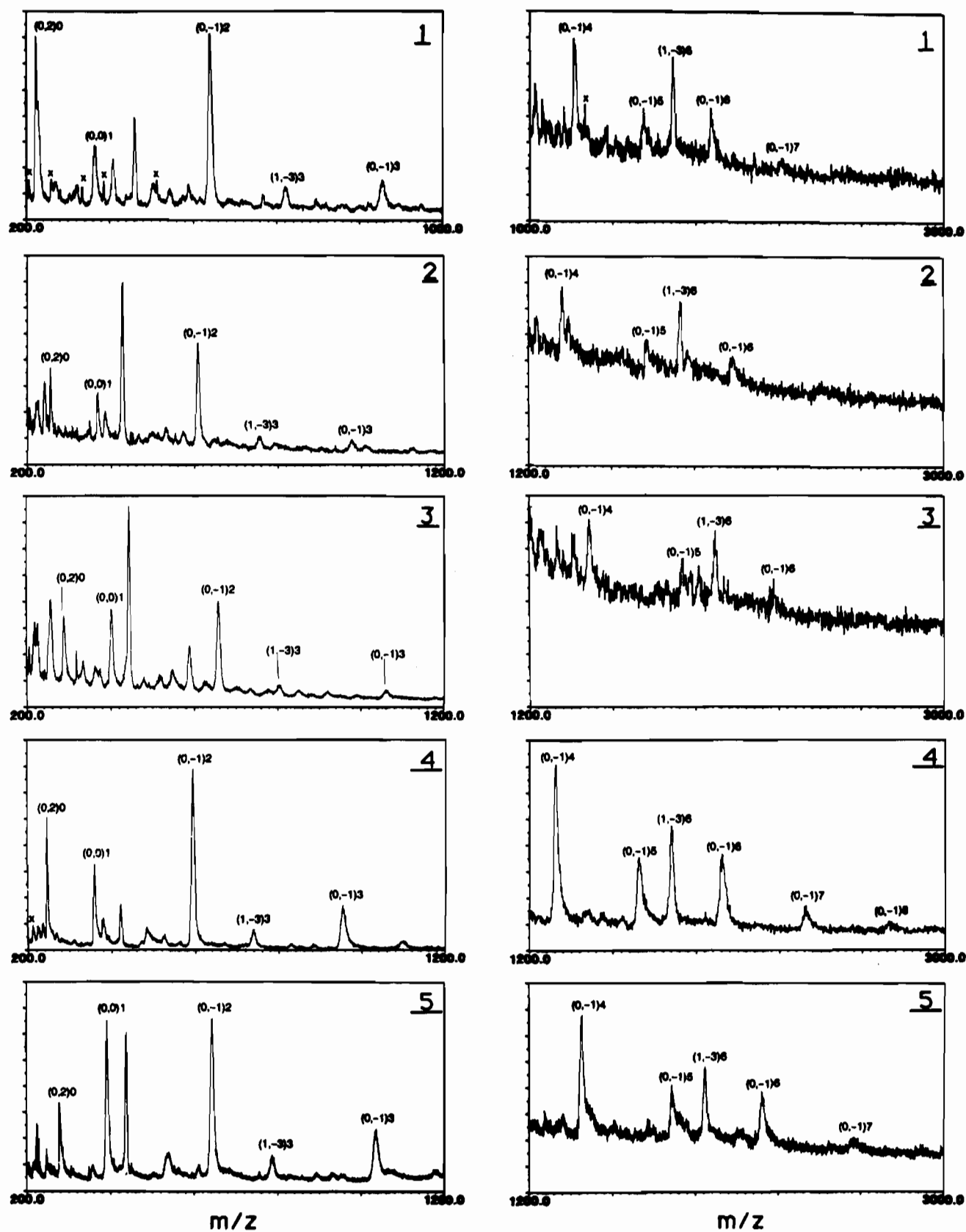


Figure 4. Medium and high mass ranges of the positive PDMS spectra of compounds 1-5.

completely covered during the electrospray process. These small differences may also be due to surface effects which vary depending on the exact amount of sample deposited during the electrospray process. No difference was observed between the electrosprayed and nitrocellulose spectra of compound 4 in the positive ionization mode.³⁵ This was not always the case as illustrated by the negative

spectrum of compound 4 where significantly more fragment ions were observed when the compound was applied to nitrocellulose (Figures 7-10) than previously observed when the sample was prepared by electrospraying³⁵ (spectrum not shown). The intense ions at m/z 268.8, 482.7, 626.5, and 770.6 were previously observed from the electrosprayed sample.³⁵

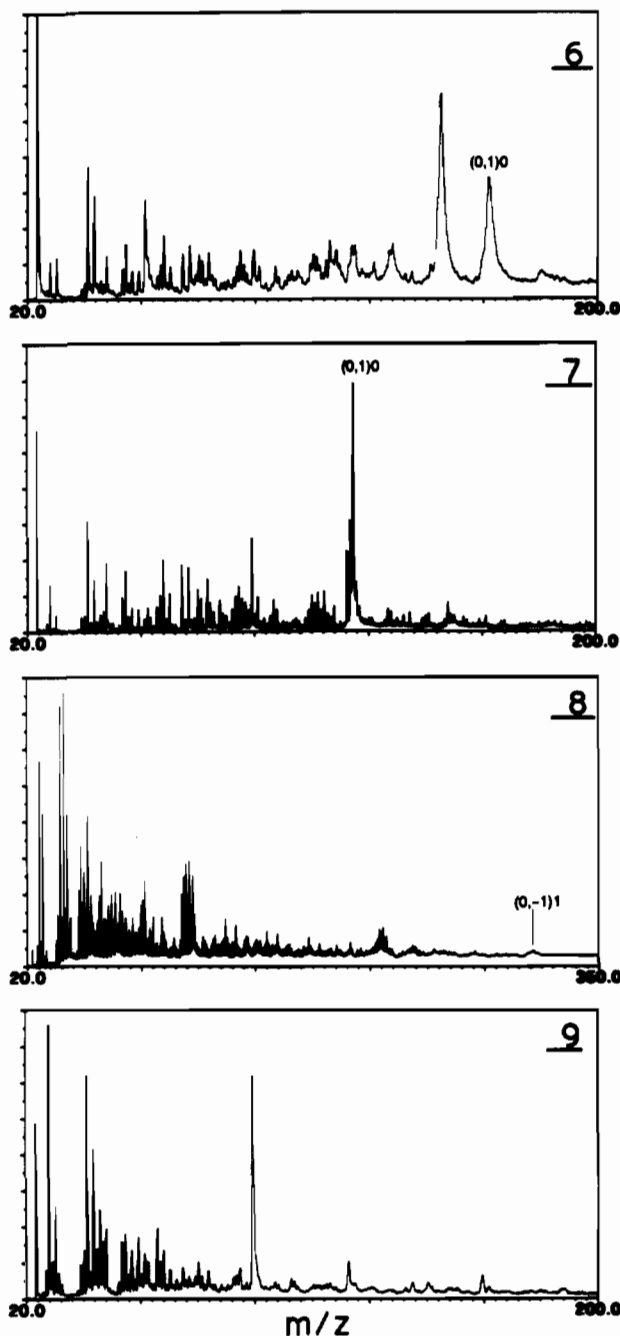


Figure 5. Low mass range of the positive PDMS spectra of compounds 6–9.

Assignment of Fragment Ions. The assignment procedures for most of the ions benefited from the fact that the spectra of compounds 1–7 are similar and the general spectral patterns are preserved both in terms of relative intensity and peak shape (see Figures 3–10). This aided substantially in resolving composition ambiguities that arose for the larger ions. Previously, we concluded that the low mass fragment ions for which the isotope distribution was sufficiently resolved were singly charged (because of the isotopic distribution and the peak spacing).³⁶ Since no evidence for multiply charged low mass fragment ions was found in that investigation³⁶ or has been reported for other inorganic complexes,^{16,19} all fragment ions were interpreted as singly charged. The assigned compositions for compounds 1–8 can be divided into three classes: (A) positive and negative ions containing only Cd and SAR, or Cd, S, and SAR with the general formulation $[\text{Cd}_x\text{S}_m(\text{SAR})_{2x+n}]^{\pm}$; (B) positive and negative ions of the previous class but with some or all of the SAR ligands devoid of the substituent in the 4- (or 2-) position: (these

desubstituted ligands are denoted SAR'); (C) positive and negative ions containing Ar and Ar' groups without S, or, in the case of 2 and 3, with F or Cl atoms in excess of the initial stoichiometry.

Proton Transfer Reactions. As shown in detail for compound 2,³⁶ comparison of the isotope distribution of some low mass fragment ions indicates that single proton transfer process can occur when these samples are analyzed using PDMS. Since we have not interpreted the assigned formula in terms of single proton transfers in Tables 1–9, these type processes may be responsible for some of the deviation between observed and calculated masses. However, we have no evidence that would support a process which involved multiple proton transfers. Therefore differences between observed and calculated masses greater than ± 1 Da are not attributed to proton transfer processes.

Assignment of Fragment Ions Involving Extensive Rearrangement. The fragment assignments proposed for ions which involved more extensive chemical rearrangement relied on the very similar appearance of the spectra, in particular the spectra of compounds 2 and 3. The procedure we used first assigned those fragment ions in the spectra of compounds 2 and 3 which were found in the spectra of compounds 1–7 as outlined above. Further comparison revealed a number of fragment ions in the spectrum of 2 whose mass corresponded with unassigned fragment ions in the spectrum of 3 shifted 16, 32, or 48 Da to higher mass. These pairs of ions (from compounds 2 and 3) were assumed to have the same composition with the exception of F atoms being replaced with Cl atoms. Therefore the mass difference indicated the number of F or Cl atoms in each fragment (i.e. a mass difference of 16 indicated one F or Cl atom, while a mass difference of 32 indicated two F or Cl atoms). These pairs of ions could therefore be used to infer the number of F or Cl atoms and from this information the number of intact ligands and therefore the composition of the fragment. Where appropriate similar fragments were assigned for compounds 1–7.

Assignment of Remaining Fragment Ions. Our procedure for assigning the remaining fragment ions compared the observed mass with many different possible combinations of the constituents (Cd, S, Ar). This procedure considered for a given number of Cd atoms, increasing numbers of Ar ligands (r) and S atoms (q), where $r - \Delta r < q < r + \Delta r$ and $\Delta r = 2$. Because of the significant differences between the observed and measured masses of the (0, -1) series, relatively large tolerances between calculated and observed masses were accepted with this procedure. The fragment ion assignments generated in this way are considered to be "uncertain" and are denoted in Tables 1–9 with "U" preceding the formula.

In Tables 1–9 more than one assignment is given in a number of cases. The different assignments are used to indicate possible species which may or may not be superimposed. In those cases where a positive and a negative fragment ion of similar mass were observed and we had no other information for deciding which assignment was correct, we proffer a number of alternatives. In those cases where no assignment is given, we have no logical explanation for the fragment ion. Our procedure would not enable identification of fragment compositions that no longer have any resemblance to the solid-state or solution-phase stoichiometry (e.g., compositions made up of three or more fragments of the ligand groups were not considered in the search process).

Many of the fragment ions contain S as well as SAR, and on the basis of the comparison of compounds 2 and 3 there is an appreciable number of ions in which a ligand devoid of the substituent in the 4- (or 2-) position was included, as SAR'. There are also ions in which it was necessary to propose an Ar or Ar' fragment without S. It is not possible to differentiate experimentally between SAR (or SAR') and S + Ar (or S + Ar'), and all such ambiguities are listed as SAR (or SAR'). Apart from Cd⁺ and Cd²⁺ which occur in all compounds except 6, all of the ions

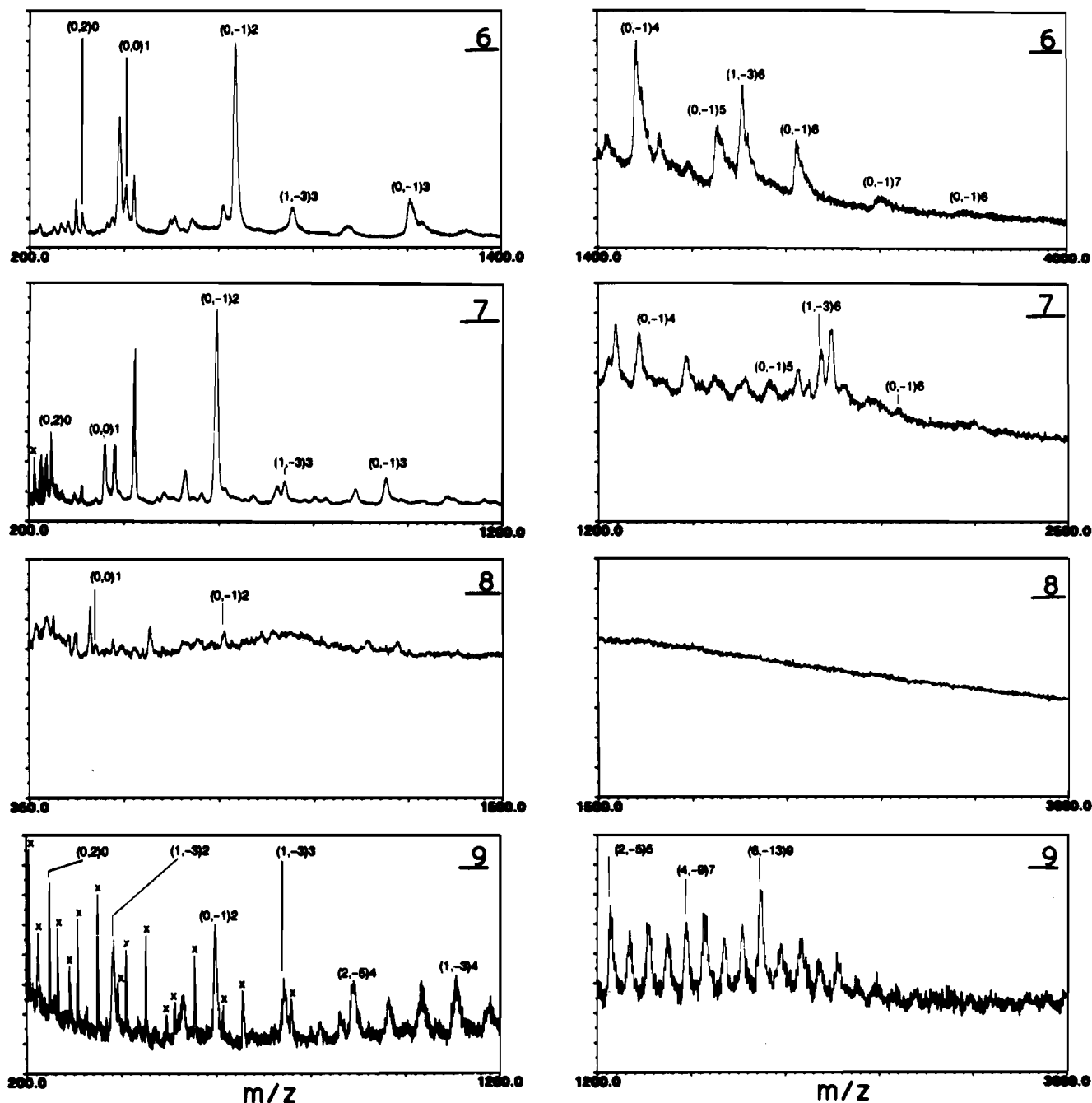


Figure 6. Medium and high mass ranges of the positive PDMS spectra of compounds 6–9.

that contain Cd also contain SAR (i.e., Cd_xS_y type ions were not observed).

Deviation between Observed and Calculated Masses. Some assignments involve significant mass discrepancies between the observed and calculated chemical atomic mass averages for a number of fragments (see Tables 1–9). For example for the $(0,-1)_6$ fragments, the mass differences for compounds 1–6 are 5.6, 2.6, 0.6, 2.8, 3.4, and 10.1 Da (although a $(0,-1)_6$ fragment was observed for compound 7 with a mass difference of 0.2 Da, the fragment ion intensity was weak and the peak shape was very broad). A number of experiments including the analysis of different thickness electrosprayed samples or the analysis of the compound applied to nitrocellulose did not reveal any significant change in the observed masses for the $(0,-1)$ fragments. Therefore the mass differences do not appear to be the result of the sample thickness as has been reported for gold clusters.⁴⁴ In comparison the $(1,-3)_6$ fragments have smaller mass differences for compounds 1–7 of 0.9, -0.2, 1.1, -2.0, 1.0, -2.4, and -0.9 Da.

Differences in Peak Shape. In addition to the differences between observed and calculated masses, there is a significant difference between the appearances of the $(0,-1)$ and the $(1,-3)$ series of fragments for compounds 1–6. In particular the $(0,-1)_6$ fragments are observed to tail to high mass while the $(1,-3)_6$ fragments are symmetric with little tailing to high or low mass. These observations can be generalized for each of the series as has been noted previously.³⁵ The fragment ion peak tailing and significant mass differences that are observed in the $(0,-1)$ series for compounds 1, 4, 5, and 6 can be explained in terms of the gaseous ions observed being created some distance from the surface. Consider the ions $Cd_4(SAR)_7$ and $Cd_5(SAR)_9$ (where $Ar = C_7H_7$) that have average masses of 1312.1 and 1670.9 Da. If the ions are formed at the surface with a potential of 20 kV and accelerated over an acceleration distance of 4.5 mm they will enter the field free region after 163.9 and 185.0 ns, respectively.

(44) Feld, H.; Leute, A.; Rading, D.; Benninghoven, A.; Schmid, G. *J. Am. Chem. Soc.* 1990, 112, 8166–8167.

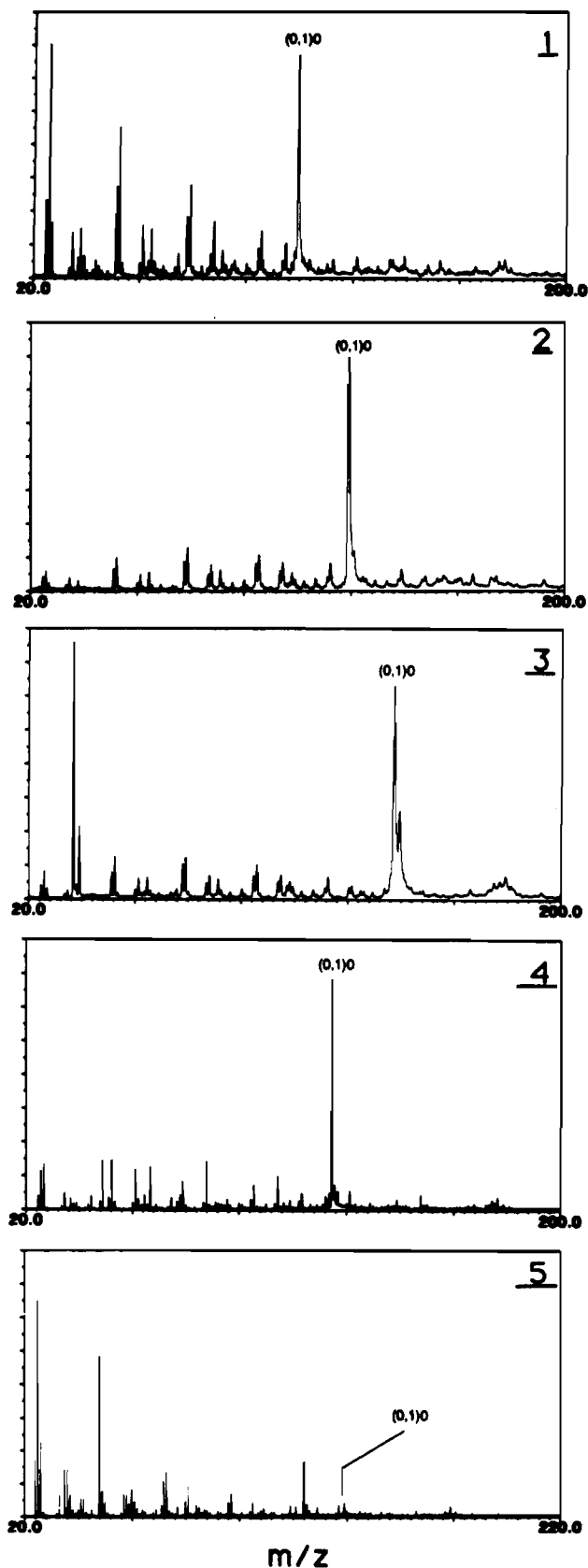


Figure 7. Low mass range of the negative PDMS spectra of compounds 1–5.

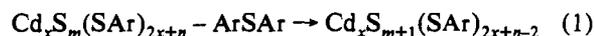
The total flight time of these ions will be 3219.9 and 3600.7 ns, respectively. In contrast, if the ions are desorbed as neutral species and ionized 33.7 μm from the surface at a potential of 19.9 kV, then the ions will spend 163.1 and 184.1 ns, respectively, in the acceleration region. As a result of the reduced energy of these ions the total flight times will increase (3226.1 and 3607.7 ns

respectively). An increase in flight time of 6.2 and 7.0 ns would result in a higher m/z ratio of 5.5 and 7.0 Da respectively. In support of this explanation, desorption of high yields of neutral amino acids and peptides have been measured following PD bombardment.⁴⁵ In addition, the similarity between the type of fragment ions formed from peptides by PD and chemical ionization⁴⁶ lends support to the idea that neutral desorption followed by a chemical ionization type process could explain gaseous ions being formed at a distance from the surface.⁴⁷ An alternative explanation, which we proposed previously for the mass difference and observed peak shape, remains equally valid.³⁵ These observations are consistent with a larger fragment ion such as $\text{Cd}_6(\text{SAr})_{10}^+$ being desorbed at the surface and eliminating $\text{Cd}_2(\text{SAr})$ at a small distance from the surface to form $\text{Cd}_4(\text{SAr})_8^+$. Similarly, the $\text{Cd}_5(\text{SAr})_9^+$ ions formed at the surface may eliminate $\text{Cd}_2(\text{SAr})$ at a small distance from the surface to form $\text{Cd}_3(\text{SAr})_7^+$ and so forth for the series of (0,–1) ions. If ions are formed at varying distances from the surface, regardless of whether a neutral fragment or a larger fragment ion is the precursor, then the observed peak shape will reflect the superposition of distributions representing ionization at varying distances away from the surface up to a maximum distance.

(A) **The Occurrence of Positive and Negative Ions $[\text{Cd}_x\text{S}_m(\text{SAr})_{2x+n}]$.** A prominent feature of the spectra is that ions in the class $[\text{Cd}_x\text{S}_m(\text{SAr})_{2x+n}]$ occur as well developed progressions of the variables m , n , and x . These progressions are accentuated by the use of the abbreviation $(m,n)_x$ defined above. The series of ions $[\text{Cd}_x\text{S}_m(\text{SAr})_{2x+n}]$ are arranged systematically in Table 10 which accounts for a total of 266 ions from the nine compounds. Also included in Table 10 are the measures of the electron populations of the positive and negative ions, expressed as Δe defined as the calculated charge (using Cd^{2+} , S^{2-} , ArS^-) less the observed charge. Ions with $\Delta e = 0$ are described as electron precise.

Electron Precise Positive Ions. The fragments assigned to the (0,–1) and (1,–3) series of electron precise (i.e., $\Delta e = 0$) positive ions are indicated in Table 10 and represent the most intense high-mass fragments observed for the six compounds 1–6 in Figures 3–10. These series extend to $x = 6$, with some (0,–1)₇ and (0,–1)₈ ions.

Positive ions of the (1,–3) series are formally derived from the (0,–1) series by loss of ArSAr . The general formalism for this is



or $(m,n)_x \rightarrow (m+1,n-2)_x$. Continuation of this ArSAr loss generates ions in the series (2,–5), (3,–7), and (4,–9), and thus there is in effect a progression of series of these ions, all of which are electron precise. In general the (2,–5) series extends from $x = 3$ to 7, while (3,–7) series ions are observed for $x = 4, 5, 7$ and (4,–9) ions are observed only for $x = 7$.

More specifically, for each compound the appearance of positive ions according to the progression of eq 1 for each value of x can be traced from Table 10. Compounds 4 and 7, both with methyl substituents, provide the largest number of members of these series, each with an almost complete progression of ions for $x = 3, 4, 5$, and some ions for the progressions with $x = 6$ and 7. Sections of the progression for $x = 3, 4, 5$ are apparent for the other compounds with aryl substituents, while in contrast, the benzyl compound 9 reveals no ions in this class other than (0,–1)₁ and (0,–1)₂. The positive and negative ions of 9 follow different progressions as described below.

(45) Sundqvist, B.; Hedin, A.; Håkansson, P.; Jonsson, G.; Salephour, M.; Sävje, G.; Roepstorff, P. *3rd International Workshop on Ion Formation from Organic Solids*; Springer Verlag, Berlin: 1985; pp 6–10.

(46) Chait, B. T.; Agosta, W. C.; Field, F. H. *Int. J. Mass Spectrom. Ion Processes* 1981, 39, 339–366.

(47) Busch, K. L.; Cooks, R. G. 1982, 218, 247–254.

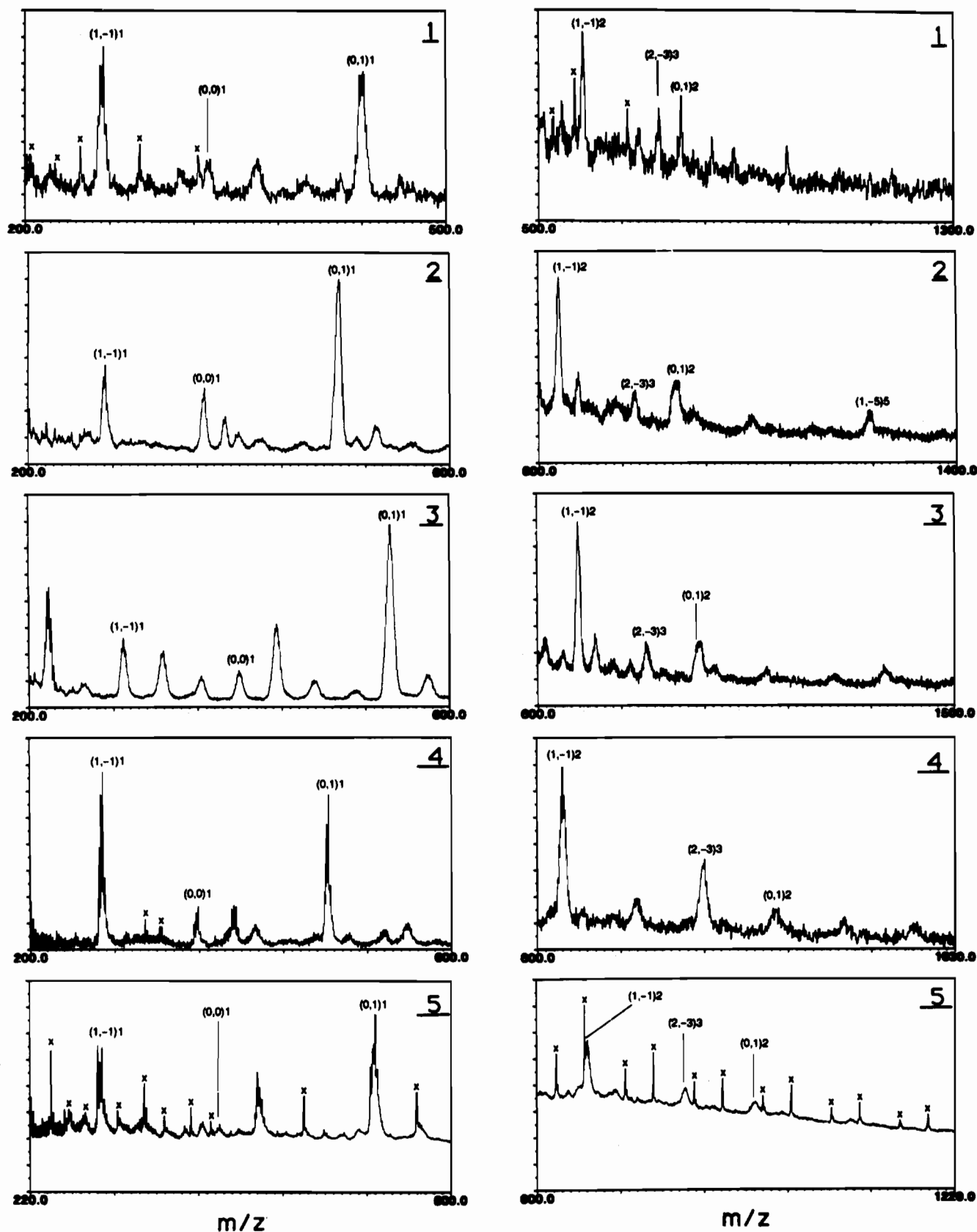


Figure 8. Medium and high mass ranges of the negative PDMS spectra of compounds 1-5.

Electron Precise Negative Ions. Electron precise negative ions occur in the series $(0,1)_{1,2,3}$, $(1,-1)_{1,2,3}$, $(2,-3)_{1,2,3,4}$, and $(3,-5)_{3,4}$ and as $(4,-7)_4$ and $(5,-9)_5$. These series are also related by the transformation of eq 1. The strongest ions occurring generally for the various compounds are $[\text{Cd}_2\text{S}(\text{SAr})_3]^-$ (i.e., $(1,-1)_2$) and $[\text{Cd}_3\text{S}_2(\text{SAr})_3]^-$ (i.e., $(2,-3)_2$).

There is a strong set of ions that are imprecise by one electron (i.e. a positive ion where $\Delta e = -1$ or a negative ion where $\Delta e = +1$). Particularly noticeable is $\text{Cd}(\text{SAr})_2$, $(0,0)_1$, that occurs in the positive and negative ion spectra of all compounds except the positive ion spectrum of 9. Formally related to these are some positive ($\Delta e = -1$) and negative ($\Delta e = +1$) ions in the $(1,-2)$

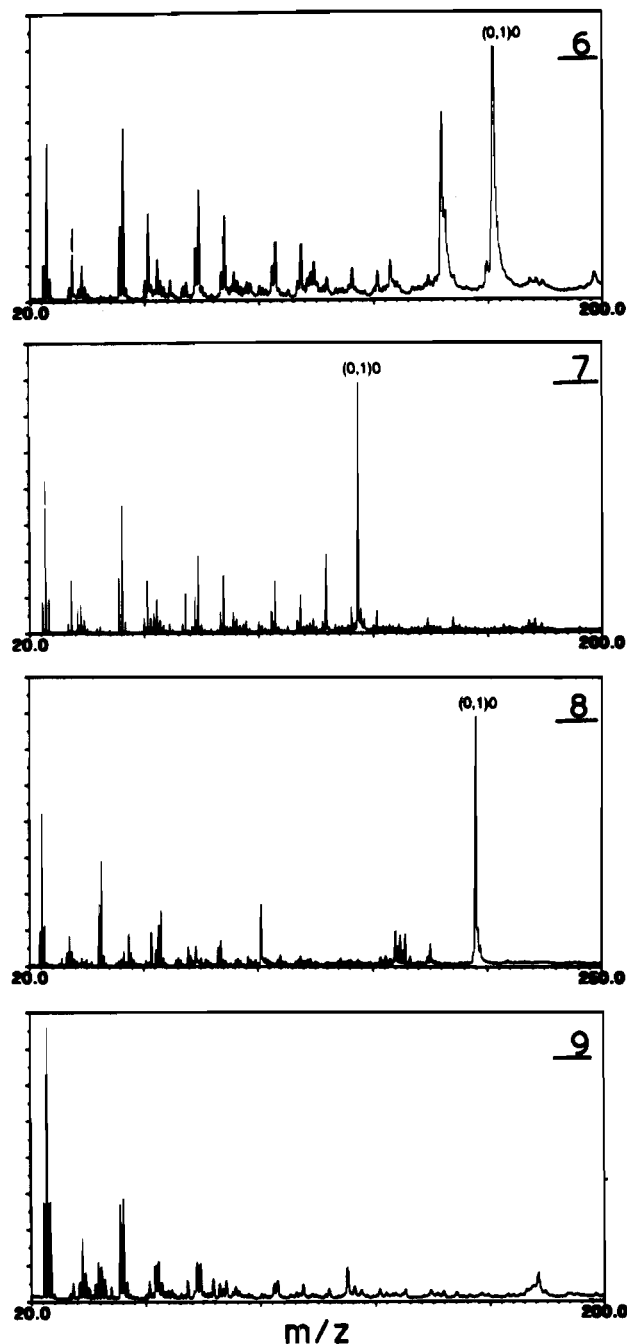


Figure 9. Low mass range of the negative PDMS spectra of compounds 6-9.

series, mainly for $x = 2$. Ions imprecise by two electrons include some negative ions ($\Delta e = +2$) of the same compositions as the dominant positive ions in the series $(0,-1)_{1,2}$, $(1,-3)_{2,3}$ and $(2,-5)_{3,4}$, and some positive ions ($\Delta e = -2$) of the same compositions as the dominant negative ions in the series $(0,1)_3$ and $(1,-1)_{1,3}$. A few other miscellaneous electron imprecise ions with small numbers of Cd atoms are included at the end of Table 10. In summary, the $(m,n)_x$ ions in class A for each $\text{Cd}(\text{SAr})_2$ compound are traced in two ways, as series variable in x or as series variable in m .

(B) Ions $[\text{Cd}_x\text{S}_m(\text{SAr}/\text{SAr}')_{2x+n}]$. There is a substantial number of ions that have the compositions of the ions in class A but contain some SAr' in place of SAr (where Ar' denotes the substituent depleted fragment ions, $\text{Ar}' = \text{C}_6\text{H}_4$). There are also some ions containing SAr' that do not have counterparts in class A. The correspondence and patterns of these ions are presented in Table 11. Examination of Table 11 reveals the following characteristics. (i) In almost all cases where an assignment

involves at least one SAr' ligand, at least half of the ligands are assigned to SAr' ; that is, if substituent loss occurs in one ligand, it occurs in the majority of ligands. (ii) Of those instances where a possible precursor (i.e., SAr -containing ion) was observed, the intensity of the SAr' containing ion is less than the possible precursor in most cases. (iii) On the basis of these possible precursors, it appears that charge reversal occurs in both directions. (iv) There is probably some significance in the presence of $[\text{Cd}_5\text{S}(\text{SAr})(\text{SAr}')_6]^+$ and $[\text{Cd}_7\text{S}_2(\text{SAr})_3(\text{SAr}')_6]^+$ in several compounds where the substituents have significant chemical differences and where the possible precursor ions are of weak intensity.

(C) Ions Containing Ar and Ar' Groups or F or Cl. There is a considerable number of positive and negative ions for all compounds (except 9) where Ar or Ar' are included in the formula. There may be other ions containing Ar or Ar' ligands that we have not assigned since we are unable to differentiate between SAr (or SAr') and $\text{S} + \text{Ar}$ (or $\text{S} + \text{Ar}'$).

Few of the ions for compound 8 ($\text{Ar} = \text{C}_6\text{F}_5$) follow the $(m,n)_x$ series prevalent in compounds 1-7 and 9. Only the first and second members occur for the $(0,-1)_x$ series of positive ions, while only the first two members of the $(0,1)_x$ series of negative ions are observed. There are only five ions containing S^{2-} , namely $[\text{CdS}(\text{SAr})]^-$, $[\text{Cd}_2\text{S}_2(\text{SAr}')_2]^-$, $[\text{Cd}_4\text{S}_2(\text{SAr}')_2]^{+-}$, $[\text{CdS}(\text{SAr}')_4]^{+-}$, and $[\text{Cd}_3\text{S}_4(\text{SAr})_3(\text{SAr}')^+]$, but a large number of ions containing Ar or Ar' without S. The ions are relatively small: there is only one Cd_3 ion, and three Cd_4 ions, with no ions with higher Cd content. We also note that there are many ions with few metals but with a surfeit of ligands (either SAr , SAr' , Ar, or Ar'). Only one ion containing SAr' together with Ar' appears, but there are 13 ions where SAr occurs with Ar or Ar'. Ions with increased numbers of Ar groups are observed only as negative ions.

There are some fragment ions that involve charge reversal when F was abstracted from the SC_6F_5 ligand: (i) $[\text{Cd}_2(\text{SAr})_3]$ appears as a positive ion as usual, but $[\text{Cd}_2(\text{SAr}')_3]$ is negative. (ii) $[\text{Cd}(\text{SAr})_2]$ appears as both positive and negative ions but $[\text{Cd}(\text{SAr})(\text{SAr}')]$ is a strong negative ion. (iii) $[\text{Cd}(\text{SAr})_3]$ appears as a negative ion as usual, but $[\text{Cd}(\text{SAr})(\text{SAr}')_2]$ is observed as a positive ion. Excluding those assignments that are considered uncertain (denoted by "U" in Table 8), there are only five ion compositions containing F, namely $[\text{Cd}(\text{SAr})\text{F}_2]^+$, $[\text{Cd}(\text{SAr})\text{F}_3]^+$, $[\text{Cd}(\text{SAr})(\text{Ar})\text{F}]^{+-}$, $[\text{Cd}(\text{SAr})_2\text{F}]^{+-}$, $[\text{Cd}_2(\text{SAr})_2\text{F}]^{+-}$.

Spectra for $\text{Cd}(\text{SBz})_2$, Compound 9. The positive and negative ion spectra of the non-arenethiolate derivative, 9, are distinctly different from those of compounds 1-8. All ions contain SBz, and almost all contain an odd number of SBz ligands. Of the 24 positive ions, 21 belong to three series, with the following general formulations:

series α	$[\text{Cd}_x\text{S}_{x-3}(\text{SBz})_3]^+$
series β	$[\text{Cd}_x\text{S}_{x-2}(\text{SBz})_3]^+$
series γ	$[\text{Cd}_x\text{S}_{x-1}(\text{SBz})]^+$

or, more generally, $[\text{Cd}_x\text{S}_{x-n}(\text{SBz})_{2n-1}]^+$, $n = 3, 2, 1$. All of these positive ions are electron precise (i.e., $\Delta e = 0$). In series α all ions from $x = 3$ to $x = 11$ are observed and all are strong except $x = 8$ and 10 (m) and $x = 11$ (w). In series β all members from $x = 2$ to $x = 12$ are observed except $x = 9$; the $x = 2-5$ fragments are strong, the $x = 6-11$ fragments are medium, and the $x = 12$ fragment is weak. There are only two members of series γ , $x = 2, 3$, and both are strong fragments. The only other positive ions are $[\text{Cd}_9\text{S}_{10}(\text{SBz})_3]^+$ (s) $\Delta e = -6$, $[\text{Cd}_2(\text{SBz})_2]^+$ (w) $\Delta e = +1$, and the unassigned fragment of 816.8 Da. The negative ions for compound 9 also fit a series:

series δ	$[\text{Cd}_x\text{S}_{x-3}(\text{SBz})_6]^-$
series ϵ	$[\text{Cd}_x\text{S}_{x-1}(\text{SBz})_3]^-$
series ϕ	$[\text{Cd}_x\text{S}_x(\text{SBz})]^-$

Series ϵ and ϕ are electron precise, $\Delta e = 0$, while series δ is electron imprecise with $\Delta e = +1$. Series ϵ has only three members,

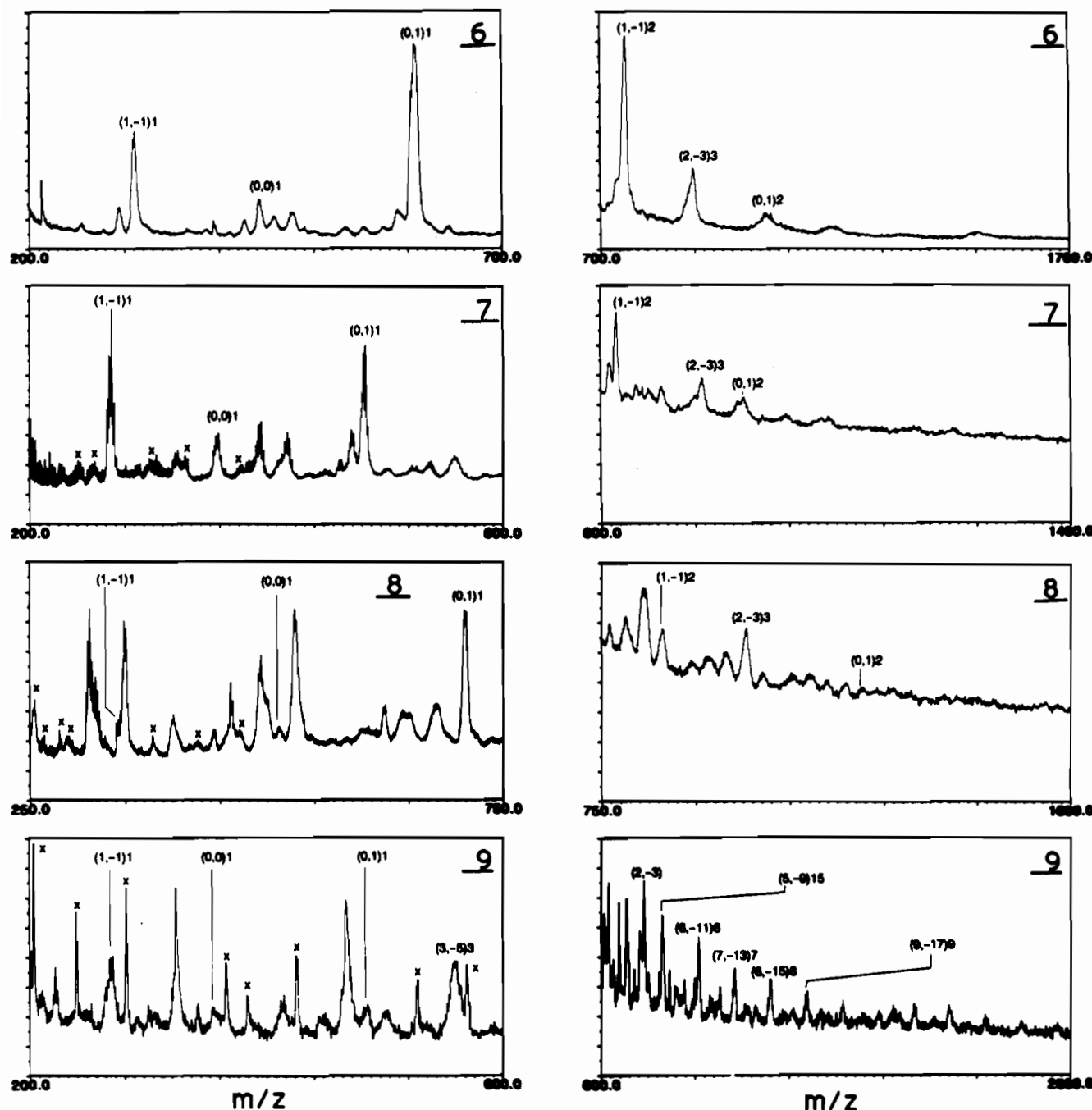


Figure 10. Medium and high mass ranges of the negative PDMS spectra of compounds 6–9.

$x = 1$ (m), 2 (w), and 3 (s), but series ϕ is extensive, from $x = 1$ to $x = 13$, with all strong fragments except for $x = 2$ and $x = 9$ –13. Series δ has six members, $x = 3, 4, 5, 7, 8, 9$, with medium or weak intensities. There are seven other miscellaneous negative ions, with less than three Cd atoms, and all are electron imprecise. Note that there are no ions with $n = 2$. The extended series (α) to (ϕ) of positive and negative ions are unusual. Whereas the first few members of series such as these can be traced for the other $\text{Cd}(\text{SAr})_2$ compounds, they do not dominate the spectra of 1–8 as they do for 9. Further, the positive ion spectrum of 9 does not contain the (0,–1) series of ions that is prominent in the spectra of 1–7. In addition, for $\text{Cd}(\text{SBz})_2$ the loss of $\text{C}_6\text{H}_5\text{CH}_2^+$ and the loss of $\text{C}_6\text{H}_5\text{CH}_2\text{SCH}_2\text{C}_6\text{H}_5$ are expected to be facile processes. For these reasons, and also because there are no evident intensity preferences in any of the series, we propose that the members of the series α to γ are the remnants of extensive BzSBz loss from the ions of series (0,–1) as shown in eqs 2–4 respectively, while series ϵ to ϕ are the remnants of extensive BzSBz loss from the ions of series (0,1) as shown in eqs 5–7 respectively.

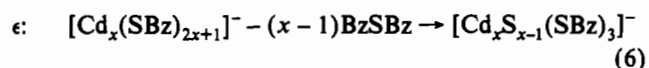
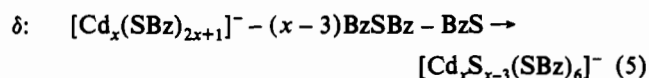
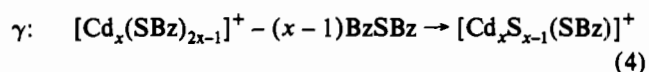
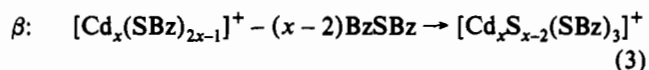
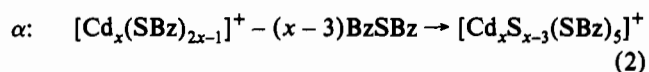


Table 1. Positive (p) and Negative (n) PD Mass Spectral Data for Compound 1, $^+[\text{Cd}(\text{SC}_6\text{H}_5)_2]$

obsd ^a				calcd		b	formula ^c	series
p		n		chem at. wt av	most intense isotopomer			
m/z	intens	m/z	intens					
109.0*	s	109.0*	s	109.17	109.01		SAr	(0,1) ₀
113.8*	m			112.42	113.90		Cd	
141.0	s			141.24	140.98		S(SAr)	(1,1) ₀
184.1	m			185.27	185.04		(SAr)Ar'	
		217.0*	w	217.33	217.02		(SAr)(SAr')	(0,2) ₀
218.2	s			218.34	218.02		(SAr) ₂	(0,2) ₀
222.9*	s			221.60	222.91		Cd(SAr)	(0,-1) ₁
225.8*	m			224.85	225.81		Cd ₂	
255.0	m	254.9*	s	253.66	254.89		CdS(SAr)	(1,-1) ₁
296.9	m			297.69	298.95		Cd(SAr)Ar'	
		308.8	m					
331.0*	s	330.9*	m	329.76	330.92		Cd(SAr)(SAr')	(0,0) ₁
366.6*	s	364.2	m	366.08	366.79		Cd ₂ S(SAr)	(1,-3) ₂
		399.0	w	398.15	398.76		Cd ₂ S ₂ (SAr)	(2,-3) ₂
408.8*	s			407.90	409.00		Cd(SAr) ₂ Ar	
		424.2	w	423.71	422.95		S ₃ (SAr) ₃	(3,3) ₀
		440.9*	s	439.94	440.94		Cd(SAr) ₃	(0,1) ₁
443.0	m			443.19	443.83		Cd ₂ (SAr) ₂	(0,-2) ₂
		466.6	m					
475.0	m	474.8	w	475.25	475.80		Cd ₂ S(SAr) ₂	(1,-2) ₂
510.9	m	509.6	w	510.57	510.67		Cd ₃ S ₂ (SAr)	(2,-5) ₃
		542.5	w	542.64	542.64		Cd ₃ S ₃ (SAr)	(3,-5) ₃
552.8	s			552.36	552.84		Cd ₂ (SAr) ₃	(0,-1) ₂
		568.0	m	568.20	568.83	U	CdS ₄ (SAr) ₃	(4,1) ₁
		584.9*	s	584.43	584.81		Cd ₂ S(SAr) ₃	(1,-1) ₂
654.3	w			655.06	654.54		Cd ₄ S ₃ (SAr)	(3,-7) ₄
		692.1	m	687.12	686.51		Cd ₄ S ₄ (SAr)	(4,-7) ₄
697.6	m			696.85	696.72		Cd ₃ S(SAr) ₃	(1,-3) ₃
		729.7	s	728.91	728.69		Cd ₃ S ₂ (SAr) ₃	(2,-3) ₃
		771.8	s	770.70	770.86		Cd ₃ S(SAr) ₅	(0,1) ₂
806.7	w			806.02	805.73		Cd ₃ (S(SAr)) ₄	(1,-2) ₃
		831.7	m	831.61	832.39		Cd ₃ S ₃ (SAr)	(5,-9) ₅
840.7	w			841.34	840.59		Cd ₄ S ₂ (SAr) ₃	(2,-5) ₄
859.4	w			860.42	861.47	U	Cd ₄ S ₆ (SAr) ₂	(6,-6) ₄
		876.0	m	873.40	874.56		Cd ₄ S ₃ (SAr) ₃	(3,-5) ₄
885.7	m			883.13	882.77		Cd ₃ (SAr) ₅	(0,-1) ₃
915.6	w			915.19	914.74		Cd ₃ S(SAr) ₅	(1,-1) ₃
959.8	w			957.01	957.39	U	Cd ₆ S ₂ (SAr) ₂	(2,-10) ₆
				960.27		U	Cd ₇ S ₂ (SAr)	(2,-13) ₇
				959.84		U	CdS ₆ (SAr) ₆	(6,4) ₁
		976.6	m	976.07	975.79	U	Cd ₂ S ₃ (SAr) ₆	(3,2) ₂
				976.10		U	Cd ₆ S ₆ (SAr)	(6,-11) ₆
				979.32		U	Cd ₃ S ₃ (SAr) ₅	(3,-1) ₃
1028.5	m			1027.62	1028.64		Cd ₄ S(SAr) ₅	(1,-3) ₄
1063.3	w			1062.9		U	Cd ₃ S ₂ (SAr) ₄	(2,-6) ₅
		1076.4	w	1075.52		U	Cd ₃ S ₆ (SAr) ₅	(6,-1) ₃
1138.3	w	1139.2	w	1136.79	1137.65		Cd ₄ S(SAr) ₆	(1,-2) ₄
				1140.04		U	Cd ₃ S(SAr) ₅	(1,-5) ₅
1166.4	w			1162.38		U	Cd ₃ S ₂ (SAr) ₄	(2,-6) ₅
				1172.10	1172.52		Cd ₃ S ₂ (SAr) ₅	(2,-5) ₅
		1180.4	w	1178.61		U	Cd ₇ S ₂ (SAr) ₃	(2,-11) ₇
				1181.43		U	Cd ₂ S ₆ (SAr) ₇	(6,3) ₂
				1181.86		U	Cd ₈ S ₂ (SAr) ₂	(2,-14) ₈
				1184.68		U	Cd ₃ S ₆ (SAr) ₆	(6,0) ₃
1219.0	s			1213.89	1214.69		Cd ₄ (SAr) ₇	(0,-1) ₄
1368.0	m			1358.38	1358.57		Cd ₃ S(SAr) ₇	(1,-3) ₅
1549.3	m			1544.65	1544.62		Cd ₅ (SAr) ₉	(0,-1) ₅
1690.1	s			1689.15	1689.50		Cd ₆ S(SAr) ₉	(1,-3) ₆
1880.0	m			1875.42	1875.55		Cd ₆ (SAr) ₁₁	(0,-1) ₆
2083.9	w			2080.79		U	Cd ₆ S ₃ (SAr) ₁₂	(3,0) ₆
				2080.82		U	Cd ₁₀ S ₆ (SAr) ₇	(6,-13) ₁₀
				2084.04		U	Cd ₇ S ₃ (SAr) ₁₁	(3,-3) ₇
2217.3	w			2206.19	2206.47		Cd ₇ (SAr) ₁₃	(0,-1) ₇

^a An asterisk denotes the most abundant isotopomer of a resolved isotope distribution. ^b U denotes an uncertain assignment. ^c Ar = C₆H₅ and Ar' = C₆H₄.

The interpretations implied in eqs 2–7 require that most SBz groups are equally easily eliminated (as BzSBz), except a small number (generally odd) that are retained. Thus the interpretation of series α , β , and γ could be that all SBz groups are subject to elimination as BzSBz from the parent fragments formed in the desorption process, except five SBz that are held more tightly and give rise to the ions in series α . Of these five SBz ligands,

two more can be eliminated to yield the ions in series β , and with greater difficulty two more SBz ligands can be lost to yield the two ions in series γ . A similar interpretation can be proposed for the negative ions, where all except the last SBz group are readily lost to yield series ϕ , although in three cases the SBz loss is arrested when three SBz ligands remain, thereby yielding the ions in series ϵ . We also envisage that the δ series would involve extensive

Table 2. Positive (p) and Negative (n) PD Mass Spectral Data for Compound 2, ${}^{\pm}[\text{Cd}(\text{SC}_6\text{H}_4\text{-4-F})_2]$

obsd				calcd		a	formula ^b	series
p		n		chem at. wt av	most intense isotopomer			
m/z	intens	m/z	intens					
113.8*	m			112.42	113.90		Cd	
126.9	s	127.0	s	127.16	127.00		SAr	(0,1) ₀
224.0	m			224.85	225.81		Cd ₂	
240.0	m			239.59	240.91		Cd(SAr)	(0,-1) ₁
254.4	m			254.32	254.00		(SAr) ₂	(0,2) ₀
		272.0	s	271.65	272.88		CdS(SAr)	(1,-1) ₁
367.1	m	365.9	s	366.75	367.91		Cd(SAr) ₂	(0,0) ₁
384.9	m	385.7	m	384.07	384.78		Cd ₂ S(SAr)	(1,-3) ₂
		398.5	m	398.81	399.88		CdS(SAr) ₂	(1,0) ₁
		418.9	w	417.81	418.88		CdS(SAr) ₂ F	
425.7	s			423.85	424.94		Cd(SAr)(SAr')Ar'	
		459.4	w	460.17	460.81		Cd ₂ (SAr)(SAr')	
463.9	w			462.85	463.95		Cd(SAr) ₂ Ar	
		493.1	s	493.91	494.91		Cd(SAr) ₃	(0,1) ₁
496.4	w			496.50	496.69		Cd ₃ S(SAr)	(1,-5) ₃
		519.9	w	511.24	511.78		Cd ₂ S(SAr) ₂	(1,-2) ₂
528.9	m	529.6	m	528.56	528.66		Cd ₃ S ₂ (SAr)	(2,-5) ₃
		563.3	w	561.63	561.64		Cd ₃ S ₃ (SAr)	(3,-5) ₃
570.9	m			568.33	568.82		Cd ₂ (SAr)(SAr') ₂	
		598.7	w	600.40	600.79		Cd ₂ S(SAr)(SAr') ₂	
606.4	s			606.33	606.81		Cd ₂ (SAr) ₃	(0,-1) ₂
		637.6	s	638.40	638.79		Cd ₃ S(SAr) ₃	(1,-1) ₂
		674.7	m	673.05	672.53		Cd ₄ S ₃ (SAr)	(3,-7) ₄
		693.5	w	695.50	695.82		Cd ₂ (SAr) ₂ (SAr') ₂	
		732.7	w	731.82	731.69		Cd ₃ S(SAr) ₂ (SAr')	
751.9	m	748.5	w	750.82	750.69		Cd ₃ S(SAr) ₃	(1,-3) ₃
		783.0	m	782.89	782.66		Cd ₃ S ₂ (SAr) ₃	(2,-3) ₃
791.0	w			790.59	790.85		Cd ₂ (SAr) ₃ (SAr')Ar'	
861.0	w			857.31	856.57		Cd ₄ S ₂ (SAr)(SAr') ₂	
		861.9	m	860.66	860.82		Cd ₂ (SAr) ₅	(0,1) ₂
		895.4	w	892.72	892.79		Cd ₂ S(SAr) ₅	(1,1) ₂
				895.31	894.56		Cd ₄ S ₂ (SAr) ₃	(2,-5) ₄
				897.09	896.73		Cd ₃ (SAr)(SAr') ₄	
900.2	w			973.08	972.72		Cd ₃ (SAr) ₅	(0,-1) ₃
973.9	m			1005.14	1004.69		Cd ₃ S(SAr) ₅	(1,-1) ₃
1007.5	w	1007.8	m	1007.73			Cd ₃ S ₂ (SAr) ₃	(2,-7) ₅
				1037.21	1036.66	U	Cd ₃ S ₂ (SAr) ₅	(2,-1) ₃
		1041.9	w	1041.57	1042.60		Cd ₄ S(SAr)(SAr') ₄	
				1117.57	1118.60		Cd ₄ S(SAr) ₅	(1,-3) ₄
1119.3	m			1125.28	1124.78		Cd ₃ (SAr) ₅ (SAr') ₂	
1156.7	w	1156.9	w	1157.34	1156.76		Cd ₃ (SAr) ₅ (SAr')Ar'	
1171.1	w			1165.86	1166.56		Cd ₅ (SAr) ₄ Ar	
				1166.96		U	Cd ₅ S ₃ (SAr) ₄	(3,-6) ₅
1231.4	m	1232.5	m	1227.40	1226.72		Cd ₃ (SAr) ₇	(0,1) ₃
				1229.99		U	Cd ₅ S(SAr) ₅	(1,-5) ₅
		1259.9	w	1259.47	1258.70		Cd ₅ S(SAr) ₇	(1,1) ₃
1342.0	s			1339.83	1340.63		Cd ₄ (SAr) ₇	(0,-1) ₄
1370.2	m			1370.32	1370.51		Cd ₅ S(SAr)(SAr') ₆	
1707.0	m			1706.57	1706.53	U	Cd ₅ (SAr) ₉	(0,-1) ₅
1850.9	s			1851.06	1851.41		Cd ₆ S(SAr) ₉	(1,-3) ₆
1884.5	m			1880.54		U	Cd ₄ S(SAr) ₁₁	(1,3) ₄
				1881.56	1882.30		Cd ₇ S ₂ (SAr) ₃ (SAr') ₆	
				1883.13		U	Cd ₆ S ₂ (SAr) ₉	(2,-3) ₆
2075.9	m			2073.32	2073.44		Cd ₆ (SAr) ₁₁	(0,-1) ₆
2455.2	w			2440.07	2440.35		Cd ₇ (SAr) ₁₃	(0,-1) ₇

^a U denotes an uncertain assignment. ^b Ar = C₆H₄F and Ar' = C₆H₄.

BzSBz loss, but that loss of an additional SBz group would initiate this cascade. The propensity toward α and β series for the positive ions was matched by the extensive ϕ series for the negative ions. This suggests that the BzSBz loss is facilitated for both positive and negative ions. Since the β series is considered to result from further BzSBz loss from the α series the occurrence of both α and β suggest that the ϕ series of negative ions are thermodynamically more favored than the positive ion series or that the subsequent dissociation of the ϕ series occurs at longer time intervals than sampled in this experiment.

Discussion

The spectra we observe for the ${}^{\pm}[\text{Cd}(\text{SAr})_2]$ and ${}^{\pm}[\text{Cd}(\text{SBz})_2]$ compounds evidently possess patterns in their ion

compositions, in addition to a background collection of ions where patterns are not obvious. The detectable patterns, described above, do not have preferred numbers of Cd atoms, and in particular Cd₄ ions as might have been expected from the adamantanoid cages are not more abundant than others. No marked dependence on the nature or position of the substituent on the aryl ring was observed. Therefore it is appropriate to conclude that the observed ions do not carry structural information characteristic of the solids from which they were formed. The abundance of ions containing S²⁻ is further evidence that the gaseous ions do not carry with them structural information from their solid origins.

This general lack of correlation of the PD mass spectrum with the solid-state structure raises questions about the ion formation processes in the PD of these nonmolecular type compounds. We

Table 3. Positive (p) and Negative (n) PD Mass Spectral Data for Compound 3, $[\text{Cd}(\text{SC}_6\text{H}_4\text{-4-Cl})_2]$

obsd ^a				calcd		b	formula	series
p		n		chem at. wt. av	most intense isotopomer			
m/z	intens	m/z	intens					
113.8*	m			112.42	113.90		Cd	
142.9*	s	143.2*	s	143.62	142.97		SAr	(0,1) ₀
217.6	s			216.33	216.01		(SAr') ₂	
		218.8*	s	219.71	219.00		(SAr)Ar'	
224.0	s			224.85	225.81		Cd ₂	
256.1	s			256.04	256.88		Cd(SAr)	(0,-1) ₁
288.4	s			287.23	285.95		(SAr) ₂	(0,2) ₀
		289.1	s	288.10	288.85		CdS(SAr)	(1,-1) ₁
		326.1	s	326.95	326.81		Cd(SAr)Cl ₂	
333.1	m			332.14	332.91		Cd(SAr)Ar'	
362.5	m	362.8	m	362.40	361.78		Cd(SAr)Cl ₃	
				364.20		U	Cd(SAr)(SAr')	
372.6	m			372.78	373.97		Cd(SAr')(Ar')	
400.5	s	399.1	m	399.66	399.85		Cd(SAr) ₂	(0,0) ₁
				400.53	400.75		Cd ₂ S(SAr)	(1,-3) ₂
		434.6	s	431.72	431.82	U	CdS(SAr) ₂	(1,0) ₁
				435.11	434.82		Cd(SAr) ₂ Cl	
442.4	s			440.30	440.91		Cd(SAr)(SAr')Ar'	
		470.8	m	470.56	469.79		Cd(SAr) ₂ Cl ₂	
				472.91	472.88	U	Cd(SAr)(SAr') ₂	
477.1	w			475.76	475.88		Cd(SAr) ₂ Ar'	
509.5	w	509.9	w	511.21	510.85		Cd(SAr) ₂ Ar	
516.2	m			512.95	512.66		Cd ₃ S(SAr)	(1,-5) ₃
		543.2	s	543.27	542.82		Cd(SAr) ₃	(0,1) ₁
545.8	m			544.14	543.73		Cd ₂ S(SAr) ₂	(1,-2) ₂
				545.01	544.63		Cd ₃ S ₂ (SAr)	(2,-5) ₃
		579.4	m	577.08	576.60		Cd ₃ S ₃ (SAr)	(3,-5) ₃
				581.40	581.79	U	Cd ₂ S(SAr') ₃	
586.4	s			584.79	584.79		Cd ₂ (SAr)(SAr') ₂	
		616.4	m	616.85	616.76		Cd ₂ S(SAr)(SAr') ₂	
624.6	w			623.63	622.75		Cd ₂ (SAr) ₂ Ar	
655.6	s	654.4	m	655.70	654.72		Cd ₂ (SAr) ₃	(0,-1) ₂
		688.1	s	687.76	686.70		Cd ₂ S(SAr) ₃	(1,-1) ₂
				689.50	688.50		Cd ₄ S ₃ (SAr)	(3,-7) ₄
699.3	w			697.21	696.69		Cd ₃ (SAr)(SAr') ₂	
		724.2	m	728.41	727.76		Cd ₂ (SAr) ₂ (SAr') ₂	
731.6	w			729.28	728.66	U	Cd ₃ S(SAr)(SAr') ₂	
		762.3	w	764.73	763.63		Cd ₃ S(SAr) ₂ (SAr')	
775.3	w			774.90	772.62		Cd ₃ (SAr)(Ar) ₂ Cl ₂	
800.8	m	799.0	w	800.18	798.60		Cd ₃ S(SAr) ₃	(1,-3) ₃
		834.4	m	832.25	830.57		Cd ₃ S ₂ (SAr) ₃	(2,-3) ₃
846.7	m			839.96	838.76		Cd ₂ (SAr) ₃ (SAr')Ar'	
877.0	w	870.1	w	873.77	872.54		Cd ₄ S ₂ (SAr)(SAr') ₂	
				878.09	877.73	U	Cd ₃ (SAr') ₅	
916.0	m			913.54	912.70		Cd ₃ (SAr)(SAr') ₄	
		947.3	m	942.93	940.67		Cd ₂ (SAr) ₅	(0,1) ₂
				944.67	942.48		Cd ₄ S ₂ (SAr) ₃	(2,-5) ₄
				945.60	944.67	U	Cd ₃ S(SAr)(SAr') ₄	
		980.2	w	974.99	972.64		Cd ₂ S(SAr) ₅	(1,1) ₂
				981.06	979.64	U	Cd ₃ S(SAr) ₂ (SAr') ₃	
988.5	w			987.83	985.63		Cd ₃ (SAr) ₄ Ar'	
				1055.35	1052.57		Cd ₃ (SAr) ₅	(0,-1) ₃
1058.0	m			1058.03	1058.57		Cd ₄ S(SAr)(SAr') ₄	
		1091.9	w	1087.42	1084.54		Cd ₃ S(SAr) ₅	(1,-1) ₃
1202.5	m			1199.84	1198.45		Cd ₄ S(SAr) ₅	(1,-3) ₄
		1239.7	w	1237.97	1237.42	U	Cd ₄ S ₂ (SAr) ₂ (SAr') ₃	
				1239.61	1236.61		Cd ₃ (SAr) ₅ (SAr')Ar'	
1248.0	m			1248.13	1246.41		Cd ₅ (SAr) ₄ Ar	
1317.6	m							
		1350.2	m	1342.58	1338.52		Cd ₃ (SAr) ₇	(0,1) ₃
				1348.65	1347.51	U	Cd ₄ (SAr) ₄ (SAr') ₃	
1387.9	m			1386.78	1386.48		Cd ₅ S(SAr)(SAr') ₆	
1458.1	s			1455.01	1452.42		Cd ₄ (SAr) ₇	(0,-1) ₄
1858.4	m			1854.66	1850.27		Cd ₅ (SAr) ₉	(0,-1) ₅
1893.4	w			1892.79	1890.24	U	Cd ₆ S(SAr) ₆ (SAr') ₃	
				1899.79	1899.43	U	Cd ₆ (SAr)(SAr') ₁₀	
1931.3	w			1928.25	1925.21	U	Cd ₆ S(SAr) ₇ (SAr') ₂	
				1930.92	1930.21		Cd ₇ S ₂ (SAr) ₃ (SAr') ₆	
				1935.24	1934.40	U	Cd ₆ (SAr) ₂ (SAr') ₉	
2000.3	m			1999.15	1995.14		Cd ₆ S(SAr) ₉	(1,-3) ₆
2040.0	w			2041.60	2039.30	U	Cd ₆ (SAr) ₅ (SAr') ₆	
2254.9	w			2254.32	2249.12		Cd ₆ (SAr) ₁₁	(0,-1) ₆

^a An asterisk denotes the most abundant isotopomer of a resolved isotope distribution. ^b U denotes an uncertain assignment. ^c Ar = C₆H₄Cl and Ar' = C₆H₄.

Table 4. Positive (p) and Negative (n) PD Mass Spectral Data for Compound 4, $^2_2[\text{Cd}(\text{SC}_6\text{H}_4\text{-4-CH}_3)_2]$

obsd ^a				calcd		b	formula ^c	series
p		n		chem at. wt av	most intense isotopomer			
m/z	intens	m/z	intens					
113.8*	m			112.42	113.90		Cd	
123.0*	s	123.0*	s	123.20	123.03		SAr	(0,1) ₀
225.6*	m			224.85	225.81		Cd ₂	
236.9*	m			235.62	236.93		Cd(SAr)	(0,-1) ₁
246.0*	s			246.40	246.05		(SAr) ₂	(0,2) ₀
268.8	w	268.8*	s	267.69	268.90		CdS(SAr)	(1,-1) ₁
		324.5*	w	326.76	327.99		Cd(SAr)Ar	
358.7*	s	358.7*	m	358.82	359.96		Cd(SAr) ₂	(0,0) ₁
380.6*	m	378.9	w	380.11	380.81		Cd ₂ S(SAr)	(1,-3) ₂
390.2	w	390.7*	m	390.89	391.93		CdS(SWAr) ₂	(1,0) ₁
		394.7*	w	392.88	393.86		CdS ₂ (SAr') ₂	
				395.95		U	CdS ₂ (SAr)	(5,-1) ₁
		412.6	m	412.18	412.78		Cd ₂ S ₂ (SAr)	(2,-3) ₂
422.9*	s			419.88	420.97		Cd(SAr)(SAr')Ar'	
				422.94	422.89		CdS ₂ (SAr) ₂	(2,0) ₁
472.0	w	471.9	w	468.98	469.89		CdS(SAr') ₃	
				471.24	471.86		Cd ₂ (SAr) ₂	(0,0) ₂
		482.7*	s	482.02	482.98		Cd(SAr) ₃	(0,1) ₁
484.4	m			484.01	484.91		CdS(SAr)(SAr') ₂	
500.2	w	502.6*	w	503.31	503.83		Cd ₂ S(SAr) ₂	(1,-2) ₂
523.2	m			524.60	524.68		Cd ₂ S ₂ (SAr)	(2,-5) ₃
		538.3	m	536.57	536.77		Cd ₃ (SAr)Ar'	
		557.5	m	556.66	556.65		Cd ₃ S ₃ (SAr)	(3,-5) ₃
561.9	w			562.38	562.92		Cd ₂ (SAr) ₂ Ar	
594.0	s			594.44	594.89		Cd ₂ (SAr) ₃	(0,-1) ₂
		626.5*	s	626.51	626.86		Cd ₂ S(SAr) ₃	(1,-1) ₂
		648.1	w	647.80	647.71	U	Cd ₃ S ₂ (SAr) ₂	(2,-4) ₃
669.4	w			669.09	668.56		Cd ₄ S ₃ (SAr)	(3,-7) ₄
		701.8	m	701.15	700.53		Cd ₄ S ₄ (SAr)	(4,-7) ₄
738.6	m			738.93	738.76		Cd ₃ S(SAr) ₃	(1,-3) ₃
		770.6	s	771.00	770.74		Cd ₃ S ₂ (SAr) ₃	(2,-3) ₃
780.1	w			778.70	778.92		Cd ₂ (SAr) ₃ (SAr)Ar'	
				781.77	781.86	U	Cd ₂ S ₂ (SAr) ₄	(2,0) ₂
829.3	w			830.06	829.82		Cd ₃ (SAr) ₄	(0,-2) ₃
		844.6	m	840.84	840.94		Cd ₂ (SAr) ₅	(0,1) ₂
				845.64	846.41		Cd ₃ S ₃ (SAr)	(5,-9) ₅
883.7	w			883.42	882.64		Cd ₄ S ₂ (SAr) ₃	(2,-5) ₄
		916.6	w	915.48	916.61		Cd ₄ S ₃ (SAr) ₃	(3,-5) ₄
954.4	s			953.26	952.85		Cd ₃ (SAr) ₅	(0,-1) ₃
		985.1	w	985.33	984.82		Cd ₃ S(SAr) ₅	(1,-1) ₃
1028.6	w			1027.91	1028.52		Cd ₂ S ₃ (SAr) ₃	(3,-7) ₅
1098.4	m			1097.75	1098.72		Cd ₄ S(SAr) ₅	(1,-3) ₄
1158.9	w			1161.88	1162.67	U	Cd ₄ S ₃ (SAr) ₅	(3,-3) ₄
1244.6	w			1242.24	1242.22		Cd ₃ S ₂ (SAr) ₅	(2,-5) ₅
1313.2	s			1312.08	1312.80		Cd ₄ (SAr) ₇	(0,-1) ₄
1455.8	w			1456.57	1456.68		Cd ₂ S(SAr) ₇	(1,-3) ₅
1528.8	w			1531.22	1531.35		Cd ₃ S ₄ (SAr) ₅	(4,-9) ₇
1601.8	w			1601.06	1601.55		Cd ₆ S ₂ (SAr) ₇	(2,-5) ₆
1673.7	s			1670.90	1670.76		Cd ₅ (SAr) ₉	(0,-1) ₅
1813.4	s			1815.39	1815.64		Cd ₆ S(SAr) ₉	(1,-3) ₆
2030.5	s			2029.72	2029.72		Cd ₅ (SAr) ₁₁	(0,-1) ₆
2395.7	m			2388.54	2388.68		Cd ₇ (SAr) ₁₃	(0,-1) ₇
2761.6	w			2747.36	2747.63		Cd ₆ (SAr) ₁₅	(0,-1) ₈

^a An asterisk denotes the most abundant isotopomer of a resolved isotope distribution. ^b U denotes an uncertain assignment. ^c Ar = C₇H₇ and Ar' = C₆H₄.

discuss this in conjunction with the geometrical and electronic structures of the cluster ions observed.

The outer track region or area surrounding the path of the PD fission fragments through the sample target (i.e., the area surrounding the infra track) which is thought to result in ionized species has not been defined. In the case of peptide or protein samples where intact desorbed molecule ions are formed, these ions originate from an area that is perturbed but not fragmented, and we may designate this as the "molecular region". Another region, presumably considerably closer to the infra track than the molecular region can be designated as the "intermediate region" (in corollary with an intermediate phase, which is intermediate in space and time but is considerably more energized than the initial solid state or the eventual distribution of gaseous ions detected). The concept of an intermediate phase has been

used for consideration of the laser ablation of metal chalcogenides, where similar populations of [M_xE_y]⁻ ions result when rather different ME compounds, and even mixtures of the elements M and E^{10,11} are ablated. An intermediate phase has also been proposed to be responsible for the formation of fullerene molecules in the PD of polyvinylidene difluoride polymers.^{48,49} In the intermediate region the degree of disruption of the solid will be extreme. Since for the cadmium thiolate compounds we do not observe [Cd_xS_y]^{+,-} ions which would require drastic rearrangement, we believe that our experiments are not sampling from the

(48) Feld, H.; Zurmühlen, R.; Leute, A.; Benninghoven, A. *J. Phys. Chem.* **1990**, *94*, 4595.

(49) Brinkmalm, G.; Barofsky, D.; Demirev, P.; Fenyö, D.; Håkansson, P.; Johnson, R.; Reinmann, C. T.; Sunqvist, B. U. R. *Chem. Phys. Lett.* **1992**, *191*, 345-.

Table 5. Positive (p) and Negative (n) PD Mass Spectral Data for Compound 5, ${}_{112}^{m}[\text{Cd}(\text{SC}_6\text{H}_4\text{-4-OCH}_3)_2]$

obsd ^a				calcd		b	formula ^c	series
p		n		chem av. wt av	most intense isotopomer			
m/z	intens	m/z	intens					
113.8*	m			112.42	113.90		Cd	
		124.0*	s	124.16	124.00		SAr''	
139.0*	s	139.0	m	139.20	139.02		SAr	(0,1) ₀
225.6*	m			224.85	225.81		Cd ₂	
246.9*	m			247.36	247.03		(SAr)(SAr')	
252.8*	w			251.62	252.93		Cd(SAr)	(0,-1) ₁
278.2*	s			278.40	278.04		(SAr) ₂	(0,2) ₀
281.1*	w	280.8*	s	280.39	279.97		S(SAr'') ₂	
285.9*	w	285.0*	s	283.69	284.90		CdS(SAr)	(1,-1) ₁
357.8	m	358.8*	w	358.75	359.98		Cd(SAr)Ar	
				359.18	360.93		Cd(SAr)(SAr')	
		376.0*	w	375.78	376.92		Cd(SAr)(SAr'')	
391.8*	s	390.9*	w	390.82	391.95		Cd(SAr) ₂	(0,0) ₁
396.9*	m			396.11	396.80		Cd ₂ S(SAr)	(1,-3) ₂
		424.8*	s	422.88	423.92		CdS(SAr) ₂	
439.2*	s			437.94	438.89	U	CdS ₃ (SAr)(C ₇ H ₆)	
				440.14	440.86		Cd ₂ (SAr)Ar'	
		502.9*	w	501.04	501.86		CdS ₂ (SAr') ₃	
				503.24	503.85	U	Cd ₂ (SAr) ₂	(0,-2) ₂
		516.9*	w	514.99	515.95	U	Cd(SAr)(SAr'')	
				516.24	516.89		Cd ₂ (SAr)(Ar') ₂	
		530.9*	s	530.02	530.97		Cd(SAr) ₃	(0,1) ₁
537.5	m			540.60	540.68		Cd ₃ S ₂ (SAr)	(2,-5) ₃
563.5	w			562.08	562.94		CdS(SAr) ₃	(1,1) ₁
		572.7*	m	572.66	572.65		Cd ₃ S ₃ (SAr)	(3,-5) ₃
611.5	m			610.38	610.90		Cd ₂ (SAr) ₂ Ar	
642.9	s			642.44	642.87		Cd ₂ (SAr) ₃	(0,-1) ₂
		674.8*	s	674.50	674.85		Cd ₃ S(SAr) ₃	(1,-1) ₂
		707.5	w	706.57	706.82	U	Cd ₂ S ₂ (SAr) ₃	(2,-1) ₂
				707.76	707.78		Cd ₃ (SAr) ₂ Ar''	
		716.3	m	717.15	716.52		Cd ₄ S ₄ (SAr)	(4,-7) ₄
787.0	m			786.93	786.75		Cd ₃ S(SAr) ₃	(1,-3) ₃
		818.7	s	818.99	818.72		Cd ₃ S ₂ (SAr) ₃	(2,-3) ₃
		850.3	w	849.99	849.68		Cd ₃ S(SAr'') ₃ (SAr')	
				851.06	850.69	U	Cd ₃ S ₃ (SAr) ₃	(3,-3) ₃
894.1	w			894.06	893.80		Cd ₃ (SAr) ₄	(0,-2) ₂
		922.3	s	920.84	920.92		Cd ₂ (SAr) ₅	(0,1) ₂
932.2	w			931.42	930.62		Cd ₄ S ₂ (SAr) ₃	(2,-5) ₄
953.7	w	953.2	w	952.90	952.89		Cd ₂ S(SAr) ₅	(1,1) ₂
		963.1	w	963.48	964.60		Cd ₄ S ₃ (SAr) ₃	(3,-5) ₄
1034.7	s			1033.26	1032.82		Cd ₃ (SAr) ₅	(0,-1) ₃
1066.0	w	1065.5	m	1065.32	1064.79		Cd ₃ S(SAr) ₅	(1,-1) ₃
1096.2	w	1098.9	w	1097.39	1097.76	U	Cd ₃ S ₂ (SAr) ₅	(2,-1) ₃
				1100.64	1101.64		Cd ₄ S(SAr)(SAr'') ₂ (SAr')	
				1100.71	1101.62		Cd ₄ S ₂ (SAr)(SAr') ₄	
		1157.8	w	1156.23	1155.85	U	Cd ₂ S ₃ (SAr) ₆	(3,2) ₂
				1157.42		U	Cd ₃ (SAr) ₅ (SAr')	
1176.3	m			1177.75	1178.70		Cd ₄ S(SAr) ₅	(1,-3) ₄
1268.7	w			1268.91	1269.68		Cd ₄ (SAr) ₂ (SAr') ₅	
1345.6	w			1343.72	1342.84	U	Cd ₃ S(SAr) ₇	(1,1) ₃
1426.3	s			1424.08	1424.77		Cd ₄ (SAr) ₇	(0,-1) ₄
1469.7	w							
1568.9	w			1568.57	1568.64		Cd ₅ S(SAr) ₇	(1,-3) ₅
1713.5	w			1713.05	1713.52		Cd ₆ S ₂ (SAr) ₇	(2,-5) ₆
1739.8	w			1739.83	1739.81	U	Cd ₅ S ₂ (SAr) ₈	(2,-2) ₅
1818.1	s			1814.90	1814.71		Cd ₅ (SAr) ₉	(0,-1) ₅
				1820.19		U	Cd ₆ S(SAr) ₈	(1,-4) ₆
1880.2	m			1879.02	1878.66	U	Cd ₅ S ₂ (SAr) ₉	(2,-1) ₅
1960.4	s			1959.38	1959.59		Cd ₆ S(SAr) ₉	(1,-3) ₆
2120.5	w			2119.71		U	Cd ₄ (SAr) ₇	(0,-1) ₄
				2120.06	2119.88	U	Cd ₄ (SAr) ₁₂	(0,4) ₄
2209.1	m			2205.71	2205.66		Cd ₆ (SAr) ₁₁	(0,-1) ₆
2599.6	w			2596.53	2596.61		Cd ₇ (SAr) ₁₃	(0,-1) ₇

^a An asterisk denotes the most abundant isotopomer of a resolved isotope distribution. ^b U denotes an uncertain assignment. ^c Ar = C₆H₇O, Ar' = C₆H₄, and Ar'' = C₆H₄O.

intermediate region. We propose that fragment excision occurs from a domain of the solid cadmium thiolates much closer in energy content to the molecular region than the intermediate region. The distribution of fragment ions observed then would be a consequence of significant gas-phase rearrangement.

It can be asked whether the processes that occur after excision of a fragment from the solid state structure are predominantly

associative (incrementing *x*) or dissociative (decrementing *x*). Our results with **9** and the interpretation contained in eqs 2-7 (as well as eq 1) may help in the analysis of this question. Cascade loss of BzSBz may yield the observed ions containing little SBz implies that precursor fragments prior to the extensive SBz loss contained at least Cd₁₂ in the positive ion mode and Cd₁₃ in the negative ion mode. Both of these are larger numbers of Cd atoms

Table 6. Positive (p) and Negative (n) PD Mass Spectral Data for Compound 6, $^+[\text{Cd}(\text{SC}_6\text{H}_4\text{-4-C}_4\text{H}_9)_2]$

obsd ^a				calcd		b	formula ^c	series
p		n		chem at. wt av	most intense isotopomer			
m/z	intens	m/z	intens					
113.9*	m			112.42	113.90		Cd	
149.9	s	149.1	s				SAr	(0,1) ₀
165.1	s	165.3	s	165.29	165.07		S(SAr)	(1,1) ₀
		197.3	m	197.34	197.05			
		213.2	s					
223.9	w							
		254.3	m	252.65	253.88		CdS(SAr')	
277.4	w	277.6	w	277.70	278.98		Cd(SAr)	(0,-1) ₁
295.3	w	294.2	m	296.69	297.94		Cd(SAr')Ar'	
		310.5	s	309.77	309.76		CdS(SAr)	(1,-1) ₁
315.6	m			316.78	317.82	U	CdS ₃ (SAr')	
331.6	m			330.56	330.15		(SAr) ₂	(0,2) ₀
				333.01	333.81	U	Cd ₂ (SAr')	
		366.7	w					
		385.3	m	385.87	386.98		Cd(SAr)(SAr')	
395.5	w	394.2	m	394.69	394.09		S ₂ (SAr) ₂	(2,2) ₀
		410.1	w	409.11	409.84		Cd ₂ (SAr)Ar'	
426.3	s	426.1	m	426.75	426.06		S ₃ (SAr) ₂	(3,2) ₀
442.9	m	442.5	s	442.98	444.05		Cd(SAr) ₂	(0,0) ₁
		457.2	m	454.26	454.83		Cd ₂ S ₂ (SAr)	(2,-3) ₂
463.4	m			461.97	463.01		Cd(SAr)(SAr')Ar'	
		476.5	m	475.05	476.02		Cd(SAr) ₂	(1,0) ₁
		488.8	w	487.02	488.11		Cd(SAr) ₂ Ar'	
		499.3	w	498.29	498.89		Cd ₂ (SAr)(SAr')	
		533.0	m	530.35	530.86		Cd ₂ S(SAr)(SAr')	
		552.2	m	551.15	552.06		Cd(SAr) ₂ (SAr')	
555.2	w			555.41	555.96		Cd ₂ (SAr) ₂	(0,-2) ₂
567.5	w			566.68	566.73		Cd ₃ S ₂ (SAr)	(2,-5) ₃
		573.4	w	574.39	574.92		Cd ₂ (SAr)(SAr')Ar'	
		588.7	m	587.47	587.93		Cd ₂ S(SAr) ₂	(1,-2) ₂
		606.8	s	606.45	606.89		Cd ₂ (SAr)(SAr') ₂	
				608.26	609.13		Cd(SAr) ₃	(0,1) ₁
611.1	w			610.71	610.79		Cd ₃ (SAr)(SAr')	
		642.3	m	640.33	641.10		CdS(SAr) ₃	(1,1) ₁
689.9	m			688.62	689.06		Cd ₂ (SAr) ₂ Ar	
720.4	s			720.69	721.03		Cd ₂ (SAr) ₃	(0,-1) ₂
		751.1	s	752.75	753.00		Cd ₂ S(SAr) ₃	(1,-1) ₂
865.5	m			865.17	864.91		Cd ₃ S(SAr) ₃	(1,-3) ₃
		897.4	s	897.24	896.88		Cd ₂ S ₂ (SAr) ₃	(2,-3) ₃
1005.5	w							
		1052.4	s	1051.24	1051.18		Cd ₂ (SAr) ₅	(0,1) ₂
1165.2	s			1163.67	1163.08		Cd ₃ (SAr) ₅	(0,-1) ₃
				1166.12	1166.74	U	Cd ₅ (SAr) ₃ (SAr')	
1191.7	m	1190.8	m	1195.73	1195.05		Cd ₃ S(SAr) ₅	(1,-1) ₃
1308.1	w			1308.16	1308.96		Cd ₄ S(SAr) ₅	(1,-3) ₄
		1342.9	w	1340.22	1340.93		Cd ₄ S ₂ (SAr) ₅	(2,-3) ₄
1451.1	m			1452.64	1452.83		Cd ₅ S ₂ (SAr) ₅	(2,-5) ₅
		1491.5	m	1494.23	1494.23		Cd ₃ (SAr) ₇	(0,1) ₃
		1505.1	m	1505.50	1506.00	U	Cd ₄ S ₂ (SAr) ₆	(2,-2) ₄
1609.7	s			1606.65	1607.13		Cd ₄ (SAr) ₇	(0,-1) ₄
				1611.21	1610.34	U	Cd ₂ S ₂ (SAr) ₈	(2,4) ₂
1637.3	m							
1737.8	w			1737.19	1737.50		Cd ₆ S(SAr)(SAr') ₈	
				1737.06	1737.37	U	Cd ₉ S ₂ (SAr) ₄	(2,-14) ₉
				1739.87	1740.23	U	Cd ₄ (SAr) ₇ Ar	
1893.9	s			1895.63	1895.88		Cd ₆ S ₂ (SAr) ₇	(2,-5) ₆
2054.1	s			2049.63	2049.18		Cd ₅ (SAr) ₉	(0,-1) ₅
2078.9	m							
				2056.34	2056.75	U	Cd ₈ (SAr) ₇	(0,-9) ₈
2191.7	s			2194.12	2194.06		Cd ₆ S(SAr) ₉	(1,-3) ₆
2217.0	m			2221.62	2221.82	U	Cd ₈ (SAr) ₈	(0,-8) ₈
2502.7	s			2492.62	2493.23		Cd ₆ (SAr) ₁₁	(0,-1) ₆
2962.4	w			2935.60	2935.29		Cd ₇ (SAr) ₁₃	(0,-1) ₇
3416.2	w			3348.34	3348.10		Cd ₈ (SAr) ₁₅	(0,-1) ₈

^a An asterisk denotes the most abundant isotopomer of a resolved isotope distribution. ^b U denotes an uncertain assignment. ^c Ar = C₁₀H₁₃ and Ar' = C₆H₄.

per ion than are found for any of the other compounds. It could be that, in compounds 1-8 with the SAr ligands, the excess internal energy in the precursor clusters causes fragmentation at Cd-S bonds with the formation of ions containing fewer Cd, whereas in 9 the elimination of BzSBz dissipates the excess internal energy and allows retention of clusters with more Cd atoms.

Previously, Feld et al. have observed limited fragmentation from molecular positive ions [Mn(SR)_{2n}]⁺ derived from nickel alkylthiolates.³⁸ These authors observed (0,0)₄ → (1,-4)₄ processes which differ from the (0,-1)_x → (1,-3)_x → (2,-5)_x fragmentations of the cadmium thiolates. The negative ion SIMS and PDMS of molecular Ni_n(SR)_{2n} compounds contain only

Table 7. Positive (p) and Negative (n) PD Mass Spectral Data for Compound 7, $[\text{Cd}(\text{SC}_6\text{H}_4\text{-2-CH}_3)_2]$

obsd ^a				calcd		b	formula ^c	series
p		n		chem at. wt av	most intense isotopomer			
m/z	intens	m/z	intens					
113.9*	m			112.42	113.90		Cd	
123.1*	s	123.0*	s	123.20	123.03		SAr	(0,1) ₀
225.7*	m			224.85	225.81		Cd ₂	
237.0*	m			235.62	236.93		Cd(SAr)	(0,-1) ₁
246.1*	m			246.40	246.05		(SAr) ₂	(0,2) ₀
269.9*	w	268.9*	s	267.69	268.90		CdS(SAr)	(1,-1) ₁
296.0*	w			294.69	296.01		CdAr ₂	
312.0*	w			311.72	312.96		Cd(SAr)Ar'	
		332.9	w	333.01	333.81		Cd ₂ (SAr')	
359.3	m	358.9*	m	358.82	359.96		Cd(SAr) ₂	(0,0) ₁
380.8*	m			380.11	380.81		Cd ₂ S(SAr)	(1,-3) ₂
		394.9*	m	392.88	393.86		CdS ₂ (SAr') ₂	
		419.0*	m	417.89	419.04		Cd(SAr)Ar ₂	
				419.88	420.97		Cd(SAr)(SAr')Ar'	
423.0*	m			423.95	423.90	U	CdS ₂ (SAr) ₂	(2,0) ₁
		462.9*	w					
470.2	w	473.0*	m	468.98	469.89		CdS(SAr') ₃	
				471.24	471.86	U	Cd ₂ (SAr) ₂	(0,-2) ₂
		482.7*	s	482.02	482.98		Cd(SAr) ₃	(0,1) ₁
484.1	w			484.01	484.91		CdS(SAr)(SAr') ₂	
502.3	w	503.0	w	503.31	503.83		Cd ₂ S(SAr) ₂	(1,-2) ₂
		526.6	w	524.60	524.68		Cd ₃ S ₂ (SAr)	(2,-5) ₃
529.3	m			530.31	530.94		Cd ₂ (SAr)Ar ₂	
		538.8*	w	536.57	536.77		Cd ₃ (SAr)Ar'	
545.4	w			546.15	546.93		CdS ₂ (SAr) ₃	(2,1) ₁
563.1	w	562.9*	m	562.38	562.92		Cd ₂ (SAr) ₂ Ar	
594.1	s			594.44	594.89		Cd ₂ (SAr) ₃	(0,-1) ₂
614.0	w	614.8	m	613.47	613.76		Cd ₂ S(SAr) ₃	
				615.73	615.74	U	Cd ₃ S(SAr) ₂	(1,-4) ₃
		627.0*	s	626.51	626.86		Cd ₂ S(SAr) ₃	(1,-1) ₂
		659.2	m	661.76	661.72		Cd ₃ (SAr') ₃	
				658.57	658.83	U	Cd ₂ S ₂ (SAr) ₃	(2,-1) ₂
672.9	w			669.09	668.56		Cd ₄ S ₃ (SAr)	(3,-7) ₄
		704.8	m	701.15	700.53		Cd ₄ S ₄ (SAr)	(4,-7) ₄
723.3	m			723.90	723.74		Cd ₃ S(SAr) ₂ (SAr')	
				722.70	722.78	U	Cd ₂ S ₄ (SAr) ₃	(4,-1) ₂
739.1	m			738.93	738.76		Cd ₃ S(SAr) ₃	(1,-3) ₃
		772.3	s	771.00	770.74		Cd ₃ S ₂ (SAr) ₃	(2,-3) ₃
781.1	w			778.70	778.92		Cd ₂ (SAr) ₃ (SAr')Ar'	
				781.77	781.86	U	Cd ₂ S ₂ (SAr) ₄	(2,0) ₂
803.2	w			799.99	799.77		Cd ₃ (SAr) ₂ (SAr') ₂	
				803.06	802.71	U	Cd ₃ S ₃ (SAr) ₃	(3,-3) ₃
826.3	w			824.35	823.56	U	Cd ₄ S ₄ (SAr) ₂	(4,-6) ₄
		831.7	m	832.06	831.74		Cd ₃ S(SAr) ₂ (SAr') ₂	
				830.06	829.82	U	Cd ₃ (SAr) ₄	(0,-2) ₃
		842.9	m	840.84	840.94		Cd ₂ (SAr) ₅	(0,1) ₂
				883.42	882.64		Cd ₄ S ₂ (SAr) ₃	(2,-5) ₄
888.6	m			889.13	889.90	U	Cd ₃ (SAr) ₃ (Ar) ₂	
		914.8	w	915.58	916.61		Cd ₄ S ₃ (SAr) ₃	(3,-5) ₄
				953.26	952.85		Cd ₃ (SAr) ₅	(0,-1) ₃
953.7	m	985.2	w	985.33	984.82		Cd ₃ S(SAr) ₅	(1,-1) ₃
986.0	w			1027.91	1028.52		Cd ₃ S ₃ (SAr) ₃	(3,-7) ₅
1030.3	w			1097.75	1098.72		Cd ₄ S(SAr) ₅	(1,-3) ₄
1096.2	m	1131.7	w	1129.82	1130.69		Cd ₄ S ₂ (SAr) ₅	(2,-3) ₄
				1226.01	1226.61	U	Cd ₄ S ₃ (SAr) ₅	(5,-3) ₄
1227.3	m							
1247.4	s							
1312.4	s			1312.08	1312.80		Cd ₄ (SAr) ₇	(0,-1) ₄
1442.8	s			1440.34	1440.69	U	Cd ₄ S ₄ (SAr) ₇	(4,-1) ₄
1522.2	m			1520.70	1520.62	U	Cd ₅ S ₃ (SAr) ₇	(3,-3) ₅
1604.0	m			1601.06	1601.55		Cd ₆ S ₂ (SAr) ₇	(2,-5) ₆
1670.7	m			1670.90	1670.76		Cd ₅ (SAr) ₉	(0,-1) ₅
1750.5	m			1745.55	1745.43		Cd ₇ S ₃ (SAr) ₇	(3,-7) ₇
1778.7	w			1777.61	1777.40	U	Cd ₇ S ₄ (SAr) ₇	(4,-7) ₇
1814.5	s			1815.39	1815.64		Cd ₆ S(SAr) ₉	(1,-3) ₆
1842.6	s			1841.74	1842.35	U	Cd ₇ S ₆ (SAr) ₇	(6,-7) ₇
1876.6	w			1869.67	1870.37		Cd ₇ S ₂ (SAr) ₃ (SAr') ₆	
1961.4	w			1959.88	1960.51		Cd ₇ S ₂ (SAr) ₉	(2,-5) ₇
2029.9	w			2029.72	2029.72		Cd ₆ (SAr) ₁₁	(0,-1) ₆

^a An asterisk denotes the most abundant isotopomer of a resolved isotope distribution. ^b U denotes an uncertain assignment. ^c Ar = C₇H₇ and Ar' = C₆H₄.

[Ni_xS_y]⁻ ions, with an (x,y) distribution different from the [Ni_xS_y]⁻ ions obtained in the laser ablation of solid nickel sulfides.¹² Thus

the PDMS of the molecular nickel alkanethiolates and of the non-molecular cadmium arene- (and phenylmethane-) thiolates

Table 8. Positive (p) and Negative (n) PD Mass Spectral Data for Compound 8, $^n[\text{Cd}(\text{SC}_6\text{F}_5)_2]$

obsd ^a				calcd		b	formula ^c	series
+ve		-ve		chem. at. wt av	most intense isotopomer			
m/z	intens	m/z	intens					
113.8*	s			112.42	113.90		Cd	
		199.0*	s	199.12	198.96		SAr	(0,1) ₀
225.6*	m			224.85	225.81		Cd ₂	
312.7*	w	312.9*	s	311.54	312.87		Cd(SAr)	(0,-1) ₁
		318.8*	m	317.48	318.89	U	CdArF ₂	
		344.9*	m	343.61	344.84		CdS(SAr)	(1,-1) ₁
353.6	m	350.9*	s	349.54	350.89		Cd(SAr)F ₂	
367.7	m			368.54	369.86		Cd(SAr)F ₃	
		400.7	m	400.60	401.84	U	CdS(SAr)F ₃	
		443.7	m	442.97	443.77	U	Cd ₂ (SAr)F	
446.1	m			446.54	447.89		Cd(Ar) ₂	
462.2	m	461.4	s	459.61	460.86		Cd(SAr)Ar'	
		492.9	s	491.67	492.83		Cd(SAr)(SAr')	
497.4	s	499.6	m	497.60	498.86		Cd(SAr)ArF	
510.9	m	512.8	m	510.67	511.83		Cd(SAr) ₂	(0,0) ₁
		529.5	s	529.67	530.83		Cd(SAr) ₂ F	
553.2	m			553.03	553.77		Cd ₂ (SAr)Ar'	
		603.3	w	604.10	604.74		Cd ₂ (SAr)(SAr')	
605.7	w			607.67	608.86		Cd(SAr)(Ar') ₂	
		623.7	m	623.9	623.74		Cd ₂ (SAr) ₂	(0,-2) ₂
642.2	s	642.0	m	642.09	642.73		Cd ₂ (SAr) ₂ F	
		650.0	m	649.23	649.68		Cd ₂ S ₂ (SAr') ₂	
672.9	w			671.80	672.80	U	Cd(SAr)(SAr') ₂	
				671.80	672.80	U	Cd(SAr) ₃ F	
		678.7	m	677.73	678.82		Cd(SAr) ₂ Ar	
				680.09	680.73	U	Cd ₂ (SAr) ₂ F	
		710.6	s	709.79	710.80		Cd(SAr) ₃	(0,1) ₁
722.9	m			720.09	720.76		Cd ₂ (SAr)(Ar') ₂	
				722.86	723.77	U	CdS(SAr) ₃ F ₂	
758.5	m			758.09	758.76		Cd ₂ (SAr)(Ar) ₂	
		765.4	m	765.22	765.70		Cd ₂ (SAr') ₃	
791.4	w	793.6	m	790.15	790.73		Cd ₂ (SAr) ₂ Ar	
				792.92	793.74	U	CdS ₂ (SAr) ₃ F ₄	
821.6	s			822.22	822.70		Cd ₂ (SAr) ₃	(0,-1) ₂
		827.8	s	828.94	828.54		Cd ₄ (SAr)(Ar')	
				827.35	827.62	U	CdS ₄ (SAr) ₂ F ₄	
				828.15	828.72	U	Cd ₂ (SAr) ₂ ArF ₂	
		860.8	m	861.01	860.52		Cd ₄ (SAr)(SAr')	
				860.21	860.70	U	Cd ₂ (SAr) ₃ F ₂	
912.4	w	915.8	w	912.07	911.49		Cd ₄ S ₂ (SAr) ₂	(2,-6) ₄
				912.48	912.59	U	Cd ₂ S ₄ (SAr) ₃ F	
				914.85	915.79	U	Cd(SAr) ₃ ArF ₂	
940.2	m	943.1	m	940.98	941.73		CdS(SAr) ₄	(1,2) ₁
				940.57	940.63	U	Cd ₃ (SAr) ₂ ArF ₂	
				943.34	943.64	U	CdS ₂ (SAr) ₃ F ₃	
		974.4	m	972.64	972.60	U	Cd ₃ (SAr) ₃ F ₂	
				973.05	973.70	U	CdS ₂ (SAr) ₄	(2,2) ₁
				979.78	980.84		Cd(SAr)(Ar') ₄	
		1010.1	s	1008.27	1008.69	U	Cd ₂ (SAr) ₃ ArF	
				1011.85	1012.81		Cd(SAr) ₂ (Ar') ₃	
		1041.8	m	1040.34	1040.66	U	Cd ₂ (SAr) ₄ F	
				1041.14	1041.77		Cd ₂ (Ar) ₄ Ar'	
				1043.91	1044.78		Cd(SAr) ₃ (Ar') ₂	
		1093.9	w	1091.40	1091.63	U	Cd ₂ S(SAr) ₄ F ₂	
				1092.21	1092.74		Cd ₂ (SAr)(Ar) ₄	
		1126.0	w	1123.46	1123.60	U	Cd ₂ S ₂ (SAr) ₄ F ₂	
				1124.27	1124.71		Cd ₂ (SAr) ₂ (Ar) ₃	
				1126.63	1126.62	U	Cd ₃ (SAr) ₂ Ar ₂ F ₃	
		1156.5	w	1155.53	1155.58	U	Cd ₂ S ₃ (SAr) ₄ F ₃	
				1156.33	1156.68		Cd ₂ (SAr) ₃ (Ar) ₂	
1170.3	m			1169.40	1169.66		Cd ₂ (SAr) ₄ Ar'	
				1171.76	1171.56	U	Cd ₃ (SAr) ₄ F ₂	
		1189.8	m	1188.40	1188.66		Cd ₂ (SAr) ₄ Ar	
		1219.8	w	1220.46	1220.63		Cd ₂ (SAr) ₅	(0,1) ₂
1242.5	m			1243.03	1242.46		Cd ₃ S ₄ (SAr) ₃ SAr'	
		1550.0	w	1551.01	1550.49	U	Cd ₃ (SAr) ₆ F	

^a An asterisk denotes the most abundant isotopomer of a resolved isotope distribution. ^b U denotes an uncertain assignment. ^c Ar = C₆F₅ and Ar' = C₆F₄.

are quite different. This is not surprising given the difference in structure of the substrates, the established differences between nickel and cadmium in M/S/SR chemistry,^{27,50,51} and the differences in reactivities of alkane- and arenethiolates. What

is unexpected is the lesser formation of S_wM_x(SR)_y ions by M = Ni, R = alkyl than with M = Cd, R = aryl. The condensed phase chemistry shows nickel to have a greater propensity to facile S-C cleavage and formation of S_wNi_x(SR)_y clusters.⁵¹

Table 9. Positive (p) and Negative (n) PD Mass Spectral Data for Compound 9, $_{2}^{+}[\text{Cd}(\text{SCH}_2\text{C}_6\text{H}_5)_2]$

obsd ^a				calcd		b	formula ^c	series
p		n		chem. at. wt av	most intense isotopomer			
m/z	intens	m/z	intens					
113.9*	w			112.42	113.90		Cd	
247.2	s	221.2	m	246.40	246.05		(SBz) ₂	(0,2) ₀
281.9	w	267.8	s	267.69	268.90		CdS(SBz)	(1,-1) ₁
326.0	m	300.0	w	281.71	282.91		CdS(SBz)CH ₂	
381.5	s	323.2	s	299.75	300.87	U	CdS ₂ (SBz)	(2,-1) ₁
		355.4	w	326.76	327.99		Cd(SBz)Bz	
		413.2	m	358.82	359.96	U	Cd(SBz) ₂	(0,0) ₁
468.9	w	447.0	m	380.11	380.81		Cd ₂ S(SBz)	(1,-3) ₂
		467.3	s	412.18	412.78		Cd ₂ S ₂ (SBz)	(2,-3) ₂
		483.9	m	471.24	471.86	U	Cd ₂ (SBz) ₂	(0,-2) ₂
		500.3	m	482.02	482.98		Cd(SBz) ₃	(0,1) ₁
527.6	s	503.3	m	503.31	503.83	U	Cd ₂ S(SBz) ₂	(1,-2) ₂
		558.8	s	524.60	524.68		Cd ₃ S ₂ (SBz)	(2,-5) ₃
		612.1	s	556.66	556.65		Cd ₃ S ₃ (SBz)	(3,-5) ₃
		624.7	w	594.44	594.89		Cd ₂ (SBz) ₃	(0,-1) ₂
		703.3	s	615.73	615.74	U	Cd ₃ S(SBz) ₂	(1,-4) ₃
		757.8	s	626.51	626.86		Cd ₂ S(SBz) ₃	(1,-1) ₂
		772.8	s	701.15	700.53		Cd ₄ S ₄ (SBz)	(4,-7) ₄
816.8	m	772.8	s	738.93	738.76		Cd ₃ S(SBz) ₃	(1,-3) ₃
		848.5	s	771.00	770.74		Cd ₃ S ₂ (SBz) ₃	(2,-3) ₃
		903.0	m	845.64	846.41		Cd ₅ S ₅ (SBz)	(5,-9) ₅
		993.1	s	883.42	882.64		Cd ₄ S ₂ (SBz) ₃	(2,-5) ₄
		1075.6	w	904.97	904.89	U	Cd ₂ S ₂ (SBz) ₅	(2,1) ₂
		1137.9	s	953.26	952.85		Cd ₃ (SBz) ₅	(0,-1) ₃
		1224.4	m	990.13	990.28		Cd ₆ S ₆ (SBz)	(6,-11) ₆
		1282.5	s	1027.91	1028.52		Cd ₅ S ₃ (SBz) ₃	(3,-7) ₅
		1373.6	w	1076.46	1075.87		Cd ₃ (SBz) ₆	(0,0) ₃
		1428.4	m	1097.75	1098.72		Cd ₄ S(SBz) ₅	(1,-3) ₄
		1572.5	m	1134.62	1135.16		Cd ₇ S ₇ (SBz)	(7,-13) ₇
		1657.2	w	1172.40	1172.39		Cd ₆ S ₄ (SBz) ₃	(4,-9) ₆
		1718.6	m	1220.95	1221.75		Cd ₄ S(SBz) ₆	(1,-2) ₄
		1803.9	w	1242.24	1242.60		Cd ₅ S ₂ (SBz) ₅	(2,-5) ₅
		1862.2	m	1279.10	1279.03		Cd ₈ S ₈ (SBz)	(8,-15) ₈
		1943.0	m	1316.88	1317.27		Cd ₇ S ₅ (SBz) ₃	(5,-11) ₇
		2004.7	m	1365.43	1365.62		Cd ₅ S ₂ (SBz) ₆	(2,-4) ₅
		2039.33	w	1386.73	1386.47		Cd ₆ S ₃ (SBz) ₅	(3,-7) ₆
		2039.33	w	1423.59	1423.91		Cd ₉ S ₉ (SBz)	(9,-17) ₉
		2039.33	w	1461.37	1462.14		Cd ₈ S ₆ (SBz) ₃	(6,-13) ₈
		2039.33	w	1531.22	1531.35		Cd ₇ S ₄ (SBz) ₅	(4,-9) ₇
		2039.33	w	1568.08	1568.78		Cd ₁₀ S ₁₀ (SBz)	(10,-19) ₁₀
		2039.33	w	1605.86	1606.02	U	Cd ₉ S ₁₀ (SBz) ₃	(7,-15) ₉
		2039.33	w	1654.41	1654.38		Cd ₇ S ₄ (SBz) ₆	(4,-8) ₇
		2039.33	w	1675.70	1676.22		Cd ₈ S ₅ (SBz) ₅	(5,-11) ₈
		2039.33	w	1712.57	1712.66		Cd ₁₁ S ₁₁ (SBz)	(11,-21) ₁₁
		2039.33	w	1750.35	1750.89		Cd ₁₀ S ₈ (SBz) ₃	(8,-17) ₁₀
		2039.33	w	1798.90	1799.25		Cd ₈ S ₅ (SBz) ₆	(5,-10) ₈
		2039.33	w	1820.19	1820.10	U	Cd ₉ S ₆ (SBz) ₅	(6,-13) ₉
		2039.33	w	1857.06	1857.54		Cd ₁₂ S ₁₂ (SBz)	(12,-23) ₁₂
		2039.33	w	1894.84	1894.77		Cd ₁₁ S ₉ (SBz) ₃	(9,-19) ₁₁
		2039.33	w	1943.39	1943.13		Cd ₉ S ₆ (SBz) ₆	(6,-12) ₉
		2039.33	w	1964.68	1964.98	U	Cd ₁₀ S ₇ (SBz) ₅	(7,-15) ₁₀
		2039.33	w	2001.54	2001.41		Cd ₁₃ S ₁₃ (SBz)	(13,-25) ₁₃
		2039.33	w	2039.33	2039.65		Cd ₁₂ S ₁₀ (SBz) ₃	(10,-21) ₁₂
		2039.33	w	2109.17	2109.85		Cd ₁₁ S ₈ (SBz) ₅	(8,-17) ₁₁

^a An asterisk denotes the most abundant isotopomer of a resolved isotope distribution. ^b U denotes an uncertain assignment. ^c Bz = C₇H₇.

Even so, there is no evidence for desorption of any fragment containing more than approximately 13 Cd atoms, which is relatively small compared with the masses of intact biomolecules that can be ejected by plasma desorption. The reason for this could derive from the solvent sheath associated with desorbed biomolecules and aiding the dissipation of excess internal energy.⁵²

(50) Dance, I. G.; Fisher, K. J.; Lee, G. In *Metallothioneins, Synthesis, Structure and Properties of Metallothioneins, Phytochelatins and Metal Thiolate Complexes*; Stillman, M. J., Shaw, C. F., III, Suzuki, K., Eds.; VCH Publishers: New York, 1992; pp 284-345.

(51) Dance, I. G.; Fisher, K. J. *Prog. Inorg. Chem.* **1994**, *41*, 637-803.

(52) Iribarne, J. V.; Thomson, B. A. *J. Chem. Phys.* **1976**, *64*, 2287-2294.

The nonmolecular cadmium thiolate lattices contain little or no solvent, and there is no evidence for solvent (from the sample deposition procedure) in any of the desorbed ions: without such ancillary molecules to dissipate excessive internal energy the desorbed sections of the lattice are more likely to fragment during desorption. The solvent sheath mode for energy dissipation proposed with other techniques such as electrospray⁵³ would not be available for the PD of these cadmium thiolate compounds. Another reason for the difference between the sizes of the desorbed cadmium thiolate fragments and of biomolecules could be the

(53) Loo, J. A.; Edmonds, C. G.; Smith, R. D. *Science* **1990**, *248*, 201-204.

Table 10. Composition and Intensity of Fragment Ions Observed in the Positive (p) and Negative (n) PD Mass Spectra of Compounds 1–8 together with the Measure of the Electron Population (Δe) where $\Delta e = \text{Calculated Charge} - \text{Measured Charge}$

Cd	composition			fragment ion intens for compds (p, n)								Δe		series
	S	SAr		1	2	3	4	5	6	7	8	p	n	
1	0	2	s, m	m, s	s, m	s, w	m, s	m, m	m, m	-	w	-1	+1	(0,0)
1	1	2	-	-	w, m	-	-	m	-	-	-	-3	-1	(1,0)
1	1	4	-	-	-	-	-	-	-	m, -	-	-5		(1,2)
2	1	2	m, w	-	w, w	-	-	m	w, w	-	m	-1	+1	(1,-2)
2	2	5	-	-	-	-	-	-	-	-	m		-4	(2,1)
2	5	3	-	-	-	-	-	-	-	-	s, -	-10		(5,-1)
3	3	6	-	-	-	w, -	-	-	-	-	-	-7		(3,0)
4	4	1	-	m	-	m	-	m	-	-	s, -	-2	0	(4,-7)
5	1	5	w, w	-	-	-	-	-	-	-	-	+2	+4	(1,-5)
5	2	4	w, -	-	-	-	-	-	w, -	-	-	+1		(2,-6)
5	5	1	-	m	-	m	-	-	-	-	s, -		0	(5,-9)
1	0	1	s, -	m, -	m, -	w, -	w, w	m, -	w, s	-	-	0	+2	(0,-1)
2	0	3	s, -	s, -	s, -	s, -	s, -	s, -	s, -	s, -	s, -	0		(0,-1)
3	0	5	m, -	m, -	s, -	s, -	s, -	m, -	-	-	s, -	0		(0,-1)
4	0	7	s, -	s, -	s, -	s, -	s, -	s, -	-	-	-	0		(0,-1)
5	0	9	m, -	m, -	s, -	s, -	s, -	m, -	-	-	-	0		(0,-1)
6	0	11	m, -	m, -	s, -	m, -	s, -	w, -	-	-	-	0		(0,-1)
7	0	13	w, -	w, -	m, -	w, -	w, -	-	-	-	-	0		(0,-1)
8	0	15	-	-	w, -	-	w, -	-	-	-	-	0		(0,-1)
2	1	1	s, m	m, m	m, w	m, -	-	m, -	-	-	s, -	0	+2	(1,-3)
3	1	3	m, -	m, w	m, -	m, -	m, -	m, -	-	-	s, -	0	+2	(1,-3)
4	1	5	m, -	m, -	m, -	m, -	w, -	m, -	-	-	s, -	0		(1,-3)
5	1	7	m, -	-	w, -	w, -	-	-	-	-	-	0		(1,-3)
6	1	9	s, -	s, -	s, -	s, -	s, -	s, -	-	-	-	0		(1,-3)
3	2	1	m, w	m, m	m, -	m, -	w, -	-	-	-	s, -	0	+2	(2,-5)
4	2	3	w, -	-	w, -	w, -	-	m, -	-	-	s, -	0	+2	(2,-5)
5	2	5	-	-	w, -	-	m, -	-	-	-	s, -	0		(2,-5)
6	2	7	-	-	w, -	w, -	s, -	m, -	-	-	-	0		(2,-5)
7	2	9	-	-	-	-	-	w, -	-	-	-	0		(2,-5)
4	3	1	w, -	-	w, -	-	-	w, -	-	-	-	0		(3,-7)
5	3	3	-	-	w, -	-	-	w, -	-	-	s, -	0		(3,-7)
7	3	7	-	-	-	-	-	m, -	-	-	-	0		(3,-7)
7	4	5	-	-	w, -	-	-	-	-	-	s, -	0		(4,-9)
1	0	3	-	s	m, s	-	s	w, s	w, s	-	m	-2	0	(0,1)
2	0	5	-	s	w, m	-	s	-	m	w, w	-	-2	0	(0,1)
2	0	2	-	-	w, w	-	w	w, -	-	m	w, s	+1	+3	(0,-2)
3	0	4	-	-	w, -	w, -	-	m	-	-	-	+1	+3	(0,-2)
4	0	6	-	-	-	-	-	w, -	-	-	-	+1	+3	(0,-2)
1	1	3	-	-	-	-	-	m	-	-	-		-2	(1,1)
2	1	5	-	-	-	w, w	-	-	-	-	-	-4	-2	(1,1)
3	1	7	-	w	-	w, -	-	-	-	-	-	-4	-2	(1,1)
1	1	1	m, s	-	m, s	w, s	-	s	w, s	-	m	-2	0	(1,-1)
2	1	3	-	s	-	s	-	s	-	s	-	-	0	(1,-1)
3	1	5	-	w, m	-	w, m	-	-	w, w	-	-	-2	0	(1,-1)
4	1	7	-	-	-	-	-	-	w	-	-	-2	0	(1,-1)
1	2	2	-	-	s, -	-	-	-	m, -	-	-	-5		(2,0)
2	2	4	-	-	w, -	-	-	-	w, -	-	-	-5		(2,0)
2	2	3	-	-	-	-	w	-	-	-	-		-2	(2,-1)
3	2	5	-	-	-	w, w	-	-	-	-	-	-4	-2	(2,-1)
2	2	1	-	w	-	m	-	-	m	-	-	-	0	(2,-3)
3	2	3	-	s	-	m	-	s	-	s	-	-	0	(2,-3)
4	2	5	-	-	-	-	-	w	-	w	-	-	0	(2,-3)
2	3	1	-	-	-	-	-	w	-	-	-	-	-4	(3,-3)
3	3	3	-	-	-	-	w	-	-	-	-	-	-2	(3,-3)
3	3	1	-	w	-	m	-	m	-	-	-	-	0	(3,-5)
4	3	3	-	m	-	w	-	w	-	-	-	-	0	(3,-5)

^a Key: s = strong; m = medium; w = weak; - = fragment ion not observed.

number of charges on the ions. The formation of pepsin molecule ions with PD containing one to four charges⁵⁴ appears to be easily stabilized as a gas phase ion.⁵⁵ In contrast, multiply charged ions have not been observed in the PD spectra of compounds 1–9.³⁶ If

multiple charges are transferred to the lattice fragment, the absence of solvent molecules would exclude the possibility of CID reactions ejecting small solvent molecules together with a charge and thereby reducing the overall charge state.⁵⁶ As a consequence of the absence of other forms of energy relaxation these singly (or multiply) charged fragments dissociate unimolecularly or by

(54) Craig, A. G.; Engström, A.; Bennich, H.; Kamensky, I. In *35th ASMS Conference on Mass Spectrometry and Allied Topics*; Denver, CO, May 24–29, 1987; pp 528–529.

(55) Loo, J. A.; Loo, R. R. O.; Light, K. J.; Edmonds, C. G.; Smith, R. D. *Anal. Chem.* **1992**, *64*, 81–88.

(56) Ikonou, M. G.; Blades, A. T.; Kebarle, P. *Anal. Chem.* **1991**, *63*, 1989–1998.

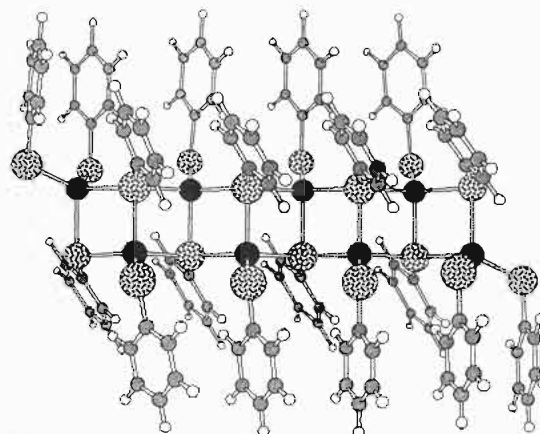
Table 11. Correlation between Intensity of One or More Positive (p) and/or Negative (n) Fragment Ions Containing Ar' groups and the Intensity of Possible Fragment Ion Precursors Containing Intact Ar Groups for Compounds 1–8^a

chem comp	precursor		comps							
	charge	observn	1	2	3	4	5	6	7	8
[Cd(SAr)(SAr')] ⁺ (0,0) ₁	p		s*							
[Cd(SAr)(SAr')] ⁻ (0,0) ₂	n		m*			w [†]	m	s		
[Cd(SAr) ₂ (SAr') ₂] ⁻ (2,0) ₁	p				w		s	m		
[Cd(SAr)(SAr') ₂] ⁺ (0,1) ₁	n							w	s	
[Cd(SAr) ₂ (SAr')] ⁻ (0,+1) ₁	n						m	s		
[CdS(SAr)(SAr')] ⁺ (1,+1) ₁	p	no				m	w		w	
[CdS(SAr')] ⁻ (1,+1) ₁	n	no				w				
[Cd ₂ (SAr')] ⁻ (0,-3) ₂	n	no						w		
[Cd ₂ (SAr)(SAr')] ⁻ (0,-2) ₂	p						w	w	w	
[Cd ₂ S(SAr)(SAr')] ⁻ (1,-2) ₂	n						m	m		
[Cd ₂ S(SAr') ₂] ⁺ (2,-2) ₂	p	no					m	w		
[Cd ₂ (SAr)(SAr') ₂] ⁺ (0,-1) ₂	p					m	s		m	s
[Cd ₂ (SAr) ₂ (SAr') ₂] ⁻ (0,0) ₂	n	no				w	m			
[Cd ₂ S(SAr') ₃] ⁺ (1,-1) ₂	p	no						w		
[Cd ₂ S(SAr)(SAr') ₂] ⁻ (1,-1) ₂	n					w				
[Cd ₂ S(SAr') ₃] ⁻ (1,-1) ₂	n								m	s
[Cd ₄ S ₂ (SAr)(SAr') ₂] ⁺ (2,-5) ₄	p		w							
[Cd ₃ (SAr)(SAr') ₄] ⁺ (0,-1) ₃	p				w	m				
[Cd ₃ (SAr) ₂ (SAr') ₂] ⁺ (0,-3) ₃	p	no				w				
[Cd ₃ S(SAr) ₂ (SAr')] ⁺ (1,-3) ₃	n					w			m	w
[Cd ₃ (SAr) ₂ (SAr') ₂] ⁺ (0,-2) ₃	n									w
[Cd ₄ (SAr) ₂ (SAr') ₃] ⁺ (0,-1) ₄	p						w*			-m
[Cd ₄ S(SAr)(SAr') ₄] ⁻ (1,-3) ₄	p					w	m			
[Cd ₄ S ₂ (SAr)(SAr') ₂] ⁻ (2,-5) ₄	n						m			
[Cd ₅ S(SAr)(SAr') ₆] ⁺ (1,-3) ₅	p	no								
[Cd ₆ S(SAr)(SAr') ₈] ⁺ (1,-3) ₆	p							w		
[Cd ₇ S ₂ (SAr) ₃ (SAr') ₆] ⁺ (2,-5) ₇	p								w	
[Cd ₇ S ₂ (SAr) ₃ (SAr') ₆] ⁻ (2,-5) ₇	n	no				m	w			

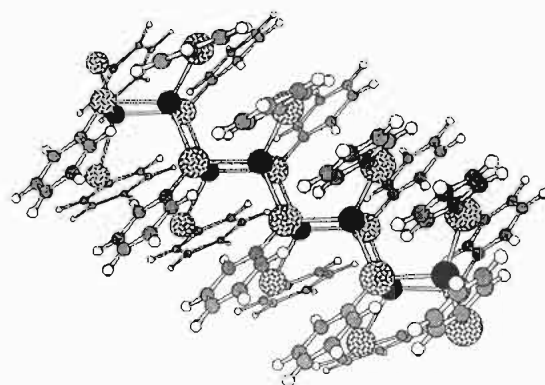
^a Fragment ions compositions and their charge are indicated by the chemical formula; precursor compositions are indicated using the (m,n)_x abbreviation; "no" in precursor observn column indicates precursor not observed for any compound. Key: s = strong; m = medium; w = weak; - indicates ion not observed; Ar' = C₇H₆ except † indicates Ar' = C₆H₄O, and * indicates Ar' = C₆H₄.

CID processes, breaking covalent bonds and ejecting small neutral (or charged) molecules such as aryl thiolate substituent groups or fragments thereof.

We have evidence for dissociative processes from large fragments initially excised from the solid state structure during



a



b

Figure 11. Postulated approximate staircase structure type illustrated by the hypothetical but energy-minimized molecule Cd₈(SPh)₁₈: (a) top view; (b) side view.

the desorption process. Our results indicate a significant delay in the formation of the (0,-1) series in terms of the observed fragment ion peak shapes and measured masses and this delay would allow considerable dissociation and/or rearrangement. On the basis of the similar patterns observed in the mass spectra, these processes would appear to involve dissociative fragmentations and rearrangements which are uniform for compounds 1–8. We note that the cluster compositions that prevail in solution, and appear to have thermodynamic stability in that they are formed in self-assembly reactions in solution, are not prevalent in our PD ion compositions: specifically [SCd₈(SAr)_{12+n}], [S₄Cd₁₀(SAr)_{12+n}], and [S₄Cd₁₇(SAr)_{24+n}]^{57–59} are not observed.

Ion Structures. The observed [Cd_xS_m(SAr)_{2x+n}][±] ions in class A belong to well-defined and general series (m,n)_x, not random distributions, an observation which leads to the expectation of principles of structure, electronic and/or geometrical, which govern the compositions of the observed ions. The generality of the ion compositions over the different compounds implies that these structure/stability principles are properties of the gaseous ions, not of the solid-state structures from which they are formed by PD. In the absence of fragmentation patterns, or of spectroscopic data, we can only speculate about the structures and the pertinent structural principles.

The known crystal structures of Cd/S/SR compounds provide guidance, and allow definition of the following relevant structural patterns:^{27,50} (a) the coordination number of Cd with thiolate

(57) Dance, I. G.; Choy, A.; Scudder, M. L. *J. Am. Chem. Soc.* **1984**, *106*, 6285.

(58) Lee, G. S. H.; Craig, D. C.; Ma, I. N. L.; Scudder, M. L.; Bailey, T. D.; Dance, I. G. *J. Am. Chem. Soc.* **1988**, *110*, 4863.

(59) Lee, G. S. H.; Fisher, K. J.; Craig, D. C.; Scudder, M. L.; Dance, I. G. *J. Am. Chem. Soc.* **1990**, *112*, 6435.

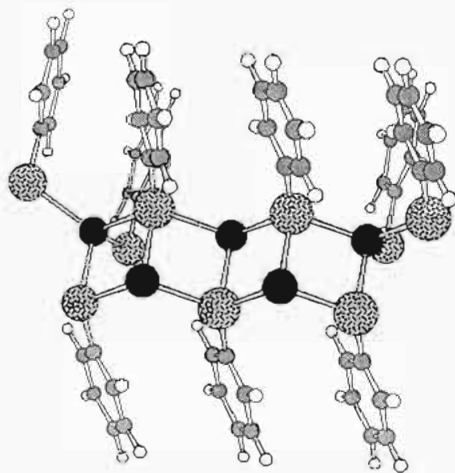


Figure 12. Postulated approximate staircase structure for the ion $\text{Cd}_5\text{-(SPh)}_9$. Other isomers are possible by relocating terminal SPh ligands onto different Cd atoms.

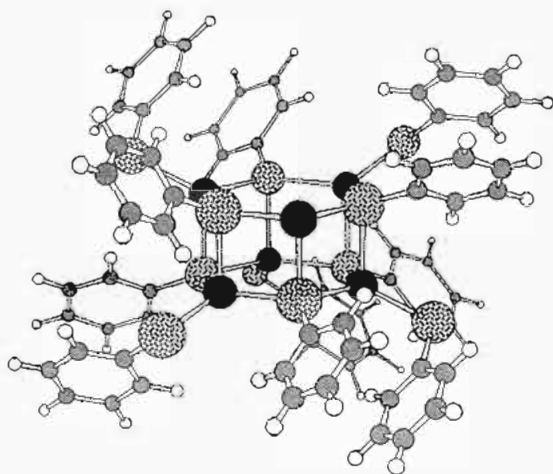


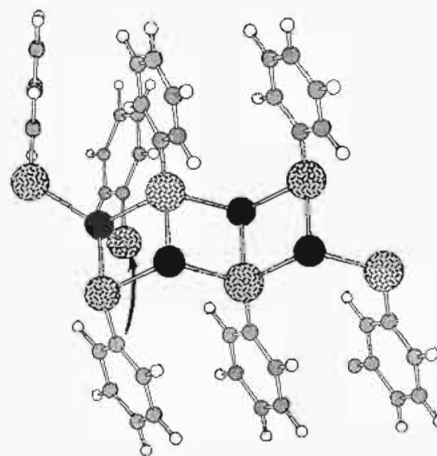
Figure 13. Energy-minimized cyclic postulate structure for the ion $\text{Cd}_6\text{-(SR)}_{11}$.

ligands is normally 4, but can be 3 or even 2 with hindered arylthiolate ligands;^{60,61} (b) SAR ligands can be terminal, doubly bridging or triply bridging, rarely quadruply bridging; (c) Ar substituents have substantial steric requirements, and there is a large difference between the steric requirements of the two types of ligands, SAR and S; (d) S ligands are usually triply-bridging or quadruply-bridging, less frequently doubly-bridging or terminal; (e) $\text{Cd}_3(\text{SAR})_3$ cycles are more prevalent than $\text{Cd}_2(\text{SAR})_2$ cycles, but the latter are known²⁷ and indeed occur in the crystal structure of 7, and are possible for the structures of the gaseous ions.

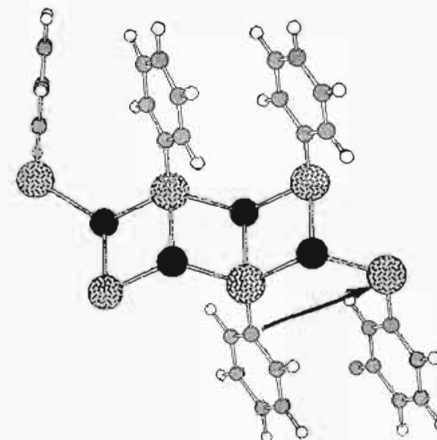
We can make some general postulates about ion structure by combining these geometrical features with the ligand/metal composition of the ions. The ligand/metal ratio is less than 2 in a majority of the ions. Therefore in order to achieve metal coordination numbers of 4 in these ions the average degree of bridging for all ligands would have to be greater than 2. Thus, to the extent that there are terminal (nonbridging) ligands on the periphery of the ions completing the four coordination of the outer metal atoms, the inner ligands will need to be at least triply bridging. There could be steric limitations for $(\mu_3\text{-SAR})$ ligands at inner positions, which will be preferentially occupied by the S atoms when present. It is also clear that many metal atoms in many of the gaseous ions will be devoid of terminal ligands and have coordination numbers less than 4.

(60) Gruff, E. S.; Koch, S. A. *J. Am. Chem. Soc.* **1990**, *112*, 1245-6.

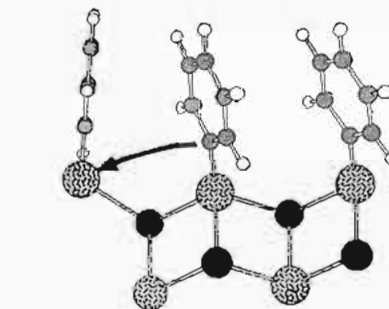
(61) Bochmann, M.; Webb, K.; Harman, M.; Hursthouse, M. B. *Angew. Chem., Int. Ed. Engl.* **1990**, *29*, 638.



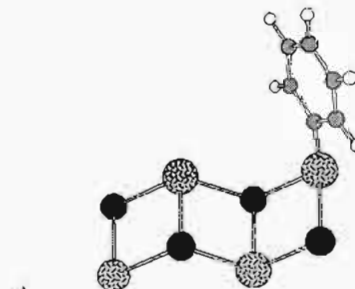
a



b



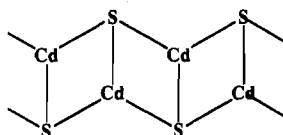
c



d

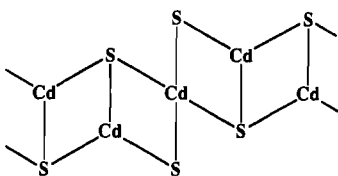
Figure 14. Postulated approximate structure for $[\text{Cd}_4(\text{SPh})_7]$ (a), and the sequence of PhSPh eliminations from vicinal ligands leading to possible structures for $[\text{Cd}_4\text{S}(\text{SAR})_5]$ (b), $[\text{Cd}_4\text{S}_2(\text{SAR})_3]$ (c), and $[\text{Cd}_4\text{S}_3(\text{SAR})]$ (d).

These precepts, together with the fact that each $(m,n)_x$ series increments ($\Delta x = \pm 1$) by addition or subtraction of $\text{Cd}(\text{SAR})_2$, lead us to postulate a linear rather than globular structural principle for the series of PD fragment ions. Globular structures, based on expanding (symmetrical) polyhedra, tend to have



10

preferred numbers of atoms. A structural framework that can provide the basis for all ions is the oligomer of edge-sharing rhombuses in zigzag or staircase motif, **10**. Key features of this structure type are illustrated in Figure 11, which shows the species $[\text{Cd}_8(\text{SPh})_{18}]^{2-}$ in its conformation energy-minimized with the force field developed for metal thiolates.⁶² There are triply-bridging SPh ligands along the extended molecule, doubly-bridging SPh at each end, and terminal SPh at each Cd atom. The aryl rings adopt the parallel configuration which maximizes the attractive dispersion forces. The $(0,-1)_8$ ion is $\text{Cd}_8(\text{SAr})_{15}$, derived from Figure 11 by removal of three terminal SAR ligands creating three-coordinate Cd atoms, which can occur at various positions along the chain. Structures for all other $\text{Cd}_x(\text{SAr})_{2x-1}$ ($(0,-1)_x$ ions are easily derived from this pattern, and as an example a staircase structure for $\text{Cd}_5(\text{SPh})_9$ is shown in Figure 12. When x is even (≥ 4) it is possible to cyclize this structure, and Figure 13 shows an energy-minimized structure for $\text{Cd}_6(\text{SPh})_{11}$. The observation that x is not markedly even in the spectra indicates that cyclic structures are not favored. There is precedent for the staircase motif in crystals of Cu(I) and Ag(I) (also d^{10}) compounds.⁶³⁻⁶⁵ and there is precedent for the cyclized structures in M/S/SR chemistry.²⁷ Another variant is the coupling of two staircase structures through a *spiro* Cd linkage, **11**, that occurs



11

in the crystal structures of **7** and of $\text{Cd}(\text{SCH}_2\text{COOEt})_2$.⁶⁶ Other geometrical isomers with precedent in metal thiolate chemistry are possible, and we have previously³⁵ shown the postulate for $\text{Cd}_6(\text{SR})_{11}$ with the same connectivity as the well-known cluster $[\text{Fe}_6\text{S}_9(\text{SR})_2]^{2-}$.^{27,50} The staircase structure accounts well for the stereochemistry and products of the RSR loss sequences, at vicinal SR ligands. Using $\text{Cd}_4(\text{SPh})_7$ as an example, Figure 14 shows that the ipso carbon atoms of R are vicinal to the S of an adjacent SP, such that little distortion is needed to eliminate RSR with the retention of a bridging S ligand. The probable

sequence of three eliminations for $\text{Cd}_4(\text{SPh})_7$ to $\text{Cd}_4\text{S}_3(\text{SPh})$ is represented in parts a-d of Figure 14. Homologous structures can be drawn for the $(0,-1)_x \rightarrow (1,-3)_x \rightarrow (2,-5)_x \rightarrow (3,-7)_x$ etc. sequences for all x .

These postulates can be applied to the structures of the majority of the ions assigned with certainty in Tables 1-9.

Electronic Structures of the Ions. Electron population is a significant characteristic of metal chalcogenide and other clusters in the solution.⁵¹ Therefore Table 10 draws attention to the electron populations of the plasma-desorbed ions, expressed as the electron imprecision Δe assuming normal oxidation states for the components. Although many of the plasma-desorbed ions are electron precise, one of the simplest ions, $\text{Cd}(\text{SAr})_2$, occurs as medium to strong electron imprecise positive and negative ions for all compounds, and a considerable number of other relatively small ions are similarly imprecise.

In general, clusters of Cd (and other four-coordinate d^{10} post-transition elements) are electron precise and have no significant M-M bonding (as assessed by M-M distances in crystals), which is expected because the M-M antibonding orbitals would be filled. However, if there is a deficiency of ligands and ligand electrons, and coordination numbers are less than 4, as in many of the proposed structures, M-M antibonding orbitals would be depleted of electrons, and some M-M bonding could be expected. This is consistent with the proposed structures, in which the Cd-Cd separations across rhombuses approach ca. 2.8 Å. In order to assess the geometrical and electronic structures of the observed ions we are undertaking density functional calculations of energy minimized geometries.

Conclusions

We propose that upon PD bombardment relatively large fragments are excised from $^n[\text{Cd}(\text{SAr})_2]$ and $^n[\text{Cd}(\text{SBZ})_2]$ and that it is from these units that the fragment ions are derived. Previous assignments of a number of different series of fragment ions with general formula $[\text{Cd}_x\text{S}_m(\text{SAr})_{2x+n}]$, have been verified and new series of fragment ions have been identified. The absence of any correlation between the composition of the fragment ions and solid-state or solution-phase cluster compositions suggests different thermodynamic constraints for the formation of these gas-phase ions. The occurrence of the different series and the absence of preferred numbers of Cd atoms indicate that the ions are formed not simply by excision from the solids but by dissociative processes from an intermediate energetic stage. We conclude that the PD fragment ions of these nonmolecular compounds carry a common structural motif which is distinct from the structures observed in the solid state. A staircase structural motif involving $\text{Cd}_2[\text{S}(\text{R})]_2$ rhombuses sharing *trans* edges can account for the compositions and transformations of the series of ions.

Acknowledgment. We are indebted to Hans Bennich of the Department of Immunology at the University of Uppsala, Sweden, for his support of this project. The measurements presented were carried out while A.G.C. was a guest researcher in that department. We would like to thank David Kinny for the computer programs used to assist in the assignment of fragment ions.

(62) Gizachew, D.; Dance, I. G. Unpublished results.

(63) Dance, I. G.; Scudder, M. L.; Fitzpatrick, L. J. *Inorg. Chem.* **1985**, *24*, 2547-50.

(64) Campbell, J. A.; Raston, C. L.; White, A. H. *Aust. J. Chem.* **1977**, *30*, 1937.

(65) Eitel, E.; Oelkrug, D.; Hiller, W.; Stahle, J. Z. *Naturforsch.* **1980**, *35B*, 1247.

(66) Dance, I. G.; Scudder, M. L.; Secomb, R. *Inorg. Chem.* **1983**, *22*, 1794-1797.